ADIABATIC PACKED COLUMN SUPERCRITICAL FLUID CHROMATOGRAPHY

A THESIS
SUBMITTED TO THE FACULTY OF
UNIVERSITY OF MINNESOTA
BY

SHAWN CHARLES HELMUELLER

IN PARTIAL FULFILLMENT OF THE REQUIREMENTS
FOR THE DEGREE OF
MASTER OF SCIENCE

ADVISOR DONALD P. POE

December 2015

Acknowledgements

I would like to thank my thesis committee; Dr. Davis for agreeing to help review my work, and Dr. Siders for patiently teaching me about thermodynamics. Thank you Dr. Poe, not only for introducing me to separation science and SFC, but for also educating me about wine and scotch, or is it whiskey? Or bourbon? I guess I still cannot tell the difference. Your guidance has helped shape my education and my career, and for that I am very grateful.

Thank you to the UMD department of chemistry and biochemistry for supporting my educational, professional, and personal goals throughout my career here. And thank you to all of the people I have come to know while I have been here.

Finally, I would like to thank my beautiful wife Emily, for her unending support and encouragement. You are always there cheering me on and you keep me motivated to succeed. Thank you, I would not have done this without you.

Dedication

The work presented in this thesis is dedicated to my family. You are always interested in what I am doing and willingly offer your advice and encouragement. And to my grandpa, you were always my biggest fan and I know how proud you would have been.

> "For a lifelong education, it is more important to understand how it works than how to do it; basics rather than recipes. Procedures will change and evolve and old recipes are soon obsolete, but the underlying mechanisms will be around for a long time."
>
> ~John Calvin Giddings

Abstract

A well-known problem in supercritical fluid chromatography is the drastic decrease in chromatographic performance at temperatures above 40°C and outlet pressures below 120 bar. This phenomenon has been attributed to isenthalpic expansion and cooling of the mobile phase and poor heat transport under these temperatures and pressures. If the temperature of the fluid does not match the temperature of the column surroundings, a radial temperature gradient forms due to heat transfer between the column and the thermal environment surrounding the column. This radial temperature gradient causes a radial fluid density profile inside the column and radial distributions in important solute parameters such as diffusion coefficients and retention factors. This ultimately results in solute band broadening and a decrease in band resolution. For this reason, method development and method transfer can be complex and the pressure-temperature region near the critical point of the mobile phase is routinely avoided. A novel dual-zone still-air column heater has been developed that can be set to match the adiabatic temperature profile of the fluid inside the column as predicted by the equation of state for the fluid. As a result, the efficiency loss associated with the formation of radial temperature gradients can be largely avoided in packed analytical scale columns. For example at 60 °C with 5% methanol modifier and a flow rate of 3mL/min, a 250mm x 4.6mm x 5μm Kinetex (Coreshell) C18 column began to lose efficiency (>25% decrease in the number of theoretical plates) at outlet pressures below 140 bar in a forced air (non-adiabatic) thermal environment. The minimum outlet pressure was decreased to 120 bar in a traditional isothermal still air (near-adiabatic) column heater and to 100 bar in the new near-ideal adiabatic still-air heater before observing excess efficiency loss. Decreasing the minimum outlet pressure from 140 bar to 120 bar and 100 bar resulted in a corresponding increase in the retention factor for n-octadecylbenzene from k=3.6 to k=5.5 and k=16.9 respectively. Simulations for the relative effect of axial gradients in the retention factor on the apparent plate height suggest that in a perfectly adiabatic environment, negligible efficiency loss should be observed. As a result, efficient separations can be carried out at higher temperatures and lower outlet pressures compared

to traditional column thermostatting techniques by operating the SFC column adiabatically.

Table of Contents

List of Tables

List of Figures

1. Introduction

Supercritical fluid chromatography (SFC) is a separation technique complementary to gas and liquid chromatography, and the mobile phase used to carry a sample through the chromatographic column differentiates one technique from the other. In gas chromatography (GC), the mobile phase is a gas. Gas mobile phases have the advantages of low viscosity and high diffusivity, which enable the use of high flow rates and long columns. This results in very fast, efficient separations. Since the solvating power of low-pressure gasses is negligible, GC is limited to low molecular weight, volatile compounds that are thermally stable in the gas phase. In high pressure liquid chromatography (HPLC), the mobile phase is a liquid. HPLC is capable of handling a much wider range of compounds compared to GC due to the increased solvating power of liquids. Flow rates for LC are much lower compared to GC due to an increase in mobile phase viscosity and a decrease in diffusivity for liquids. SFC has characteristics that are between those of GC and HPLC and uses a compressible fluid as the mobile phase. Carbon dioxide is used almost exclusively due to its low critical temperature (31^{o}C) and critical pressure (74 bar), chemical inertness, natural abundance, and net neutral environmental impact. The phase diagram for neat carbon dioxide, Figure 1, shows distinct phase boundaries when passing between solid, liquid and gaseous phases; this is true for any solvent. The phase boundaries are highlighted by solid red lines, and crossing the phase boundaries needs to be avoided in chromatographic practice [9]. Due to the gas-liquid phase boundary, there are clear distinctions between the methods and instruments used for GC and LC applications, and SFC serves as a bridge between the two.

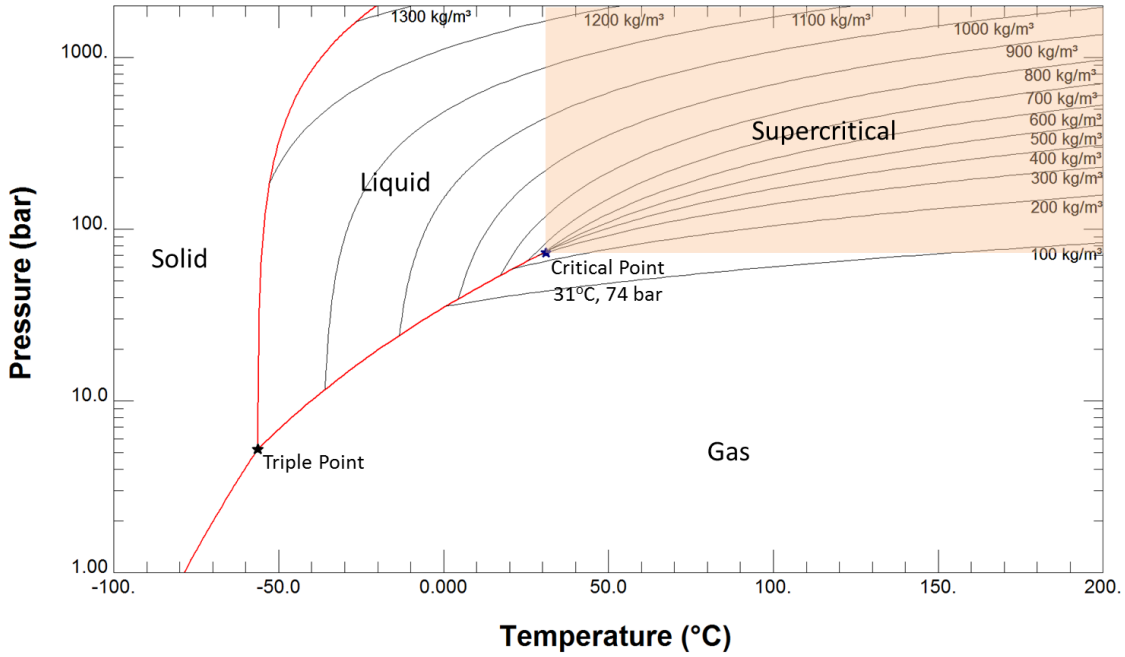

Figure 1. Phase Diagram for neat carbon dioxide showing the solid, liquid, gas, and supercritical regions. The black star marks the triple point and blue star marks the critical point. Solid red lines show phase transitions, and the solid black lines are isopycnic (constant density) lines. Generated from REFPROP data Version 9.0 [1]

Widespread implementation of SFC has suffered in the past from a lack of clarity about what exactly SFC is. While the name suggests the use of a supercritical fluid, today this is not necessarily the case. It is common to use sub-critical solvents with low viscosity in a similar fashion to HPLC [2]. SFC is commonly done at relatively low temperatures, 20°C – 40°C, and at outlet pressures well above the critical pressure to avoid the gas-liquid phase boundary and high compressibility near the critical point. Under these conditions the nonpolar CO_2 mobile phase has properties similar to those of nonpolar liquid organic solvents, Table 1. In addition, changes in temperature and pressure have very little effect on the properties of the mobile phase in this region. This type of SFC is similar in many respects to normal phase LC. Due to improvements in instrumentation and method development [3], SFC has replaced normal phase LC as the method of choice for large scale separation and purification of natural products and chiral pharmaceuticals. In addition, industrial laboratories are starting to push the implementation of SFC technology to replace reversed phase LC applications as well [3]. This is due to an increase in separation speed, resolution and throughput, a decrease in

solvent consumption and disposal costs, the net neutral environmental impact and natural abundance of reclaimed CO_2, and ease of sample recovery using SFC methods.

Even though temperature and pressure are important operating parameters in SFC, little discussion is normally provided in published work on how these parameters are determined for specific applications [5]. Most commonly the oven temperature and the outlet pressure are set, perhaps arbitrarily, and method development is composed of selecting an adequate modifier concentration and or gradient to optimize analyte retention and selectivity. This is, at least in part, because the P-T region where retention and selectivity are most sensitive to changes in temperature and pressure is also the region where drastic losses in chromatographic performance are observed, near the critical point of the mobile phase. The goal of this thesis is to develop a method for working in this region near the critical point, by operating the SFC column nearly adiabatic.

1.1 Unified Chromatography

A major advantage of SFC is the ability to tune the properties of the mobile phase using temperature and pressure (or density), due to the compressibility of the mobile phase. While low pressure gasses have almost no solvating power, the solvating power of a supercritical fluid is proportional to the density of the supercritical fluid [6].

$$\delta_{SF} = \delta_{liq}\left(\frac{\rho_{SF}}{\rho_{liq}}\right) \tag{1}$$

The Hildebrand solubility parameter for a supercritical fluid (δ_{SF}) is related to the solubility parameter of the liquid (δ_{liq}) by the ratio of the density of the supercritical fluid (ρ_{SF}) to the density of the liquid (ρ_{liq}). Most simply, the solubility parameter is a measure of the interactions or solvating properties of a fluid. Given Equation (1), as you increase density the solvating power of a supercritical mobile phase approaches the solvating power of the liquid mobile phase; under low density conditions the fluid is gas-like and under high density conditions the fluid is liquid-like. Moreover, the difference in δ between two different phases determines how a particular solute will partition between the two phases [6]. As a result, the ability to change δ in a supercritical fluid, by changing the density, allows chromatographers to control how a solute partitions between the

mobile phase and stationary phase; retention is tunable in SFC by altering the density of the fluid. Table 1 was reproduced from [6] and gives the solubility parameters for various liquids. Liquid (high density) CO_2 is similar to nonpolar organic solvents such as toluene and cyclohexane. In addition, organic modifiers such as methanol and ethanol are commonly added to increase the solvating power of CO_2 further.

Table 1. Table of solubility parameters for various liquids at 298 K, unless otherwise noted [6].

Liquid	δ, $(cal/cm^3)^{1/2}$
Water	23.4
Methanol	14.5
Ethanol	12.7
Carbon Disulfide	10.0
Toluene	8.9
Carbon Dioxide (223K)	8.9
Cyclohexane	8.2
n-Heptane	7.4
Isopentane	6.8

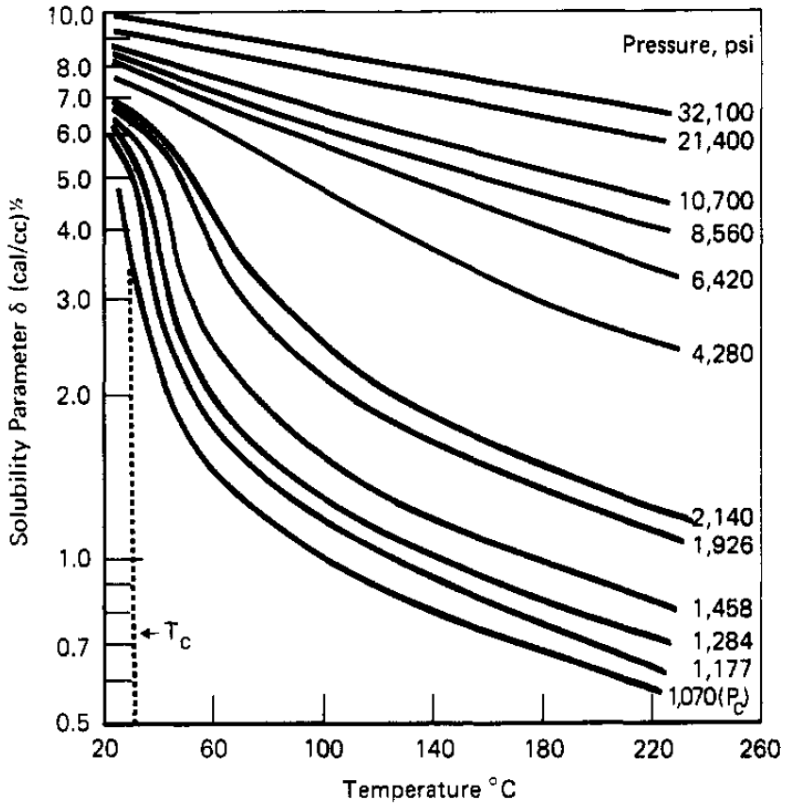

Figure 2. Effect of temperature and pressure on the solubility parameter for neat carbon dioxide. T_c is the critical temperature and P_c is the critical pressure [7].

In SFC, δ-values for neat CO_2 can range from 1.0 to 10.0 $(cal/cm^3)^{1/2}$ depending on the temperature and pressure under accessible operating conditions, and solvent strength is extremely sensitive to changes in temperature and pressure near the critical point. This is shown by the steepness of the curves in Figure 2, for conditions near the critical temperature and pressure (T_c and P_c) [7]. In principle, as long as a solute remains soluble in the mobile phase, any temperature and pressure (density) can be utilized for method development in SFC as long as phase transitions are avoided [8] and the retention factor is reasonable [8]. An example of the tunability of retention with outlet pressure is shown in Figure 3.

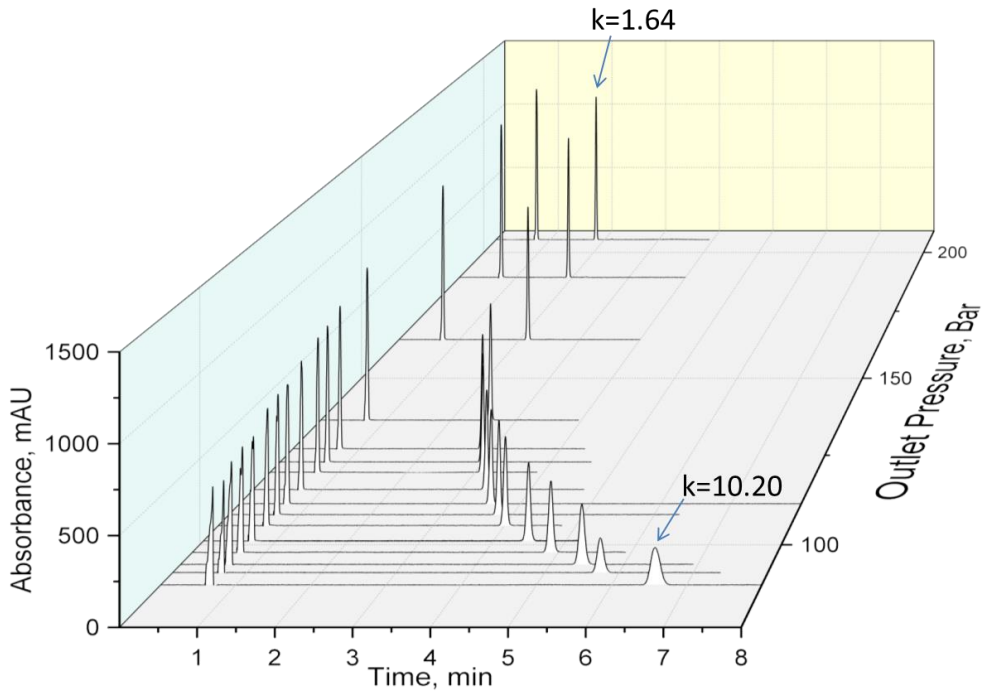

Figure 3. Effect of changing the system outlet pressure on retention for octadecylbenzene. Temperature (50 °C), flow rate (3mL/min), and modifier percentage (5% MeOH) are kept constant. Column is 250mmx4.6mmx5um Kinetex Coreshell (C18).

Pressure, or density, as a control parameter is unique to SFC. While it offers more possibilities in method development, it also provides additional complexity to the optimization process and must be chosen and controlled carefully. Density is related to temperature and pressure by the equation of state for the fluid. At any pressure above the critical pressure, the isopycnic lines in Figure 1 and Figure 4 show that the density is a continuous function from the liquid to supercritical region. Similarly, at any temperature above the critical temperature, the density is a continuous function from the gas to supercritical region. There is no abrupt change in density when passing from liquid to supercritical or from gas to supercritical. This allows chromatographers to work seamlessly across the so-called "supercritical phase boundary" without issue [9]. In fact, there are no phase boundaries for a fluid above its critical temperature. For this reason, SFC serves as a bridge between GC and LC. It is not a divergent technique. Rather, it unifies gas and liquid chromatographic techniques [6][8][9].

The idea that all three chromatographic techniques are linked together or unified through SFC has been around since the 1960s. Early work on unified chemical separation methods was done by Giddings and eventually published as a graduate text titled *Unified Separation Science*, in 1991 [6]. Chester and Parcher edited an ACS Symposium Series titled, *Unified Chromatography* in 2000 [9], which focused on theoretical aspects of unified approaches to chromatography as well as practical aspects and applications. As instrumentation has continued to improve and the need to separate more complex samples has continued to grow, the idea of a unified approach to chromatography has gained appeal in attacking complex separation hurdles once again. The two largest instrument manufacturers currently pushing the advancement of SFC technology have each incorporated this idea into their most modern SFC instruments. Agilent Technologies has recently introduced a hybrid SFC/HPLC system, *Infinity Hybrid*, that can perform both analytical scale HPLC and SFC, and Waters Corporation markets their SFC system, *Acquity UPC*^{2}, as *Convergence Chromatography*. Both speak to the unifying nature of SFC and suggest that contrary to how GC and LC have gained widespread incorporation in analytical laboratories by solving divergent separation challenges, the future widespread implementation of SFC may well depend on how robust it is in unifying gas and liquid chromatographic techniques.

1.2 Near-Critical SFC

1.2.1 Safe Zones of Operation in SFC

While there are advantages to using CO_2 as a mobile phase under sub-critical temperatures and high pressures, there are limits to the speed and resolution that can be achieved under these conditions[5][11].The most attractive region in terms of chromatographic properties (viscosity, diffusion coefficients, tunability) is in the vicinity of the critical point [5][11][12]. Unfortunately, exploration of this region is complicated by issues that arise due to mobile phase compressibility. Recent improvements in SFC pumps have solved the issue of accurately pumping compressible fluids [3], but issues related to fluid compressibility inside the chromatographic column remains a problem [5][10]-[15]. Under certain chromatographic conditions (combinations of temperature, pressure and mobile phase composition) band resolution and efficiency degrade rapidly. This complicates method development and method transfer, limits options for optimizing complex separations, and decreases the overall robustness of SFC as compared to LC. This is particularly true when using temperature and pressure as method variables. As you increase the temperature and decrease the pressure the density of the fluid decreases, and the compressibility increases. The closer you operate to the critical point, the more rapidly these properties change. This was described in great detail through a series of papers published by Guiochon and Tarafder *et. al.* [16]-[20]. The authors introduce the use of isopycnic, constant density, plots on the P-T plane to help direct method development and explain chromatographic performance for neat CO_2 and mixed mobile phases in SFC. They observed that performance deteriorates in the P-T region where the isopycnic lines are closely spaced. In this region, small changes in temperature and pressure result in large changes in fluid density. This is accompanied by poor heat transport and an overall lack of thermal equilibrium inside of the column [11][12][18][24].

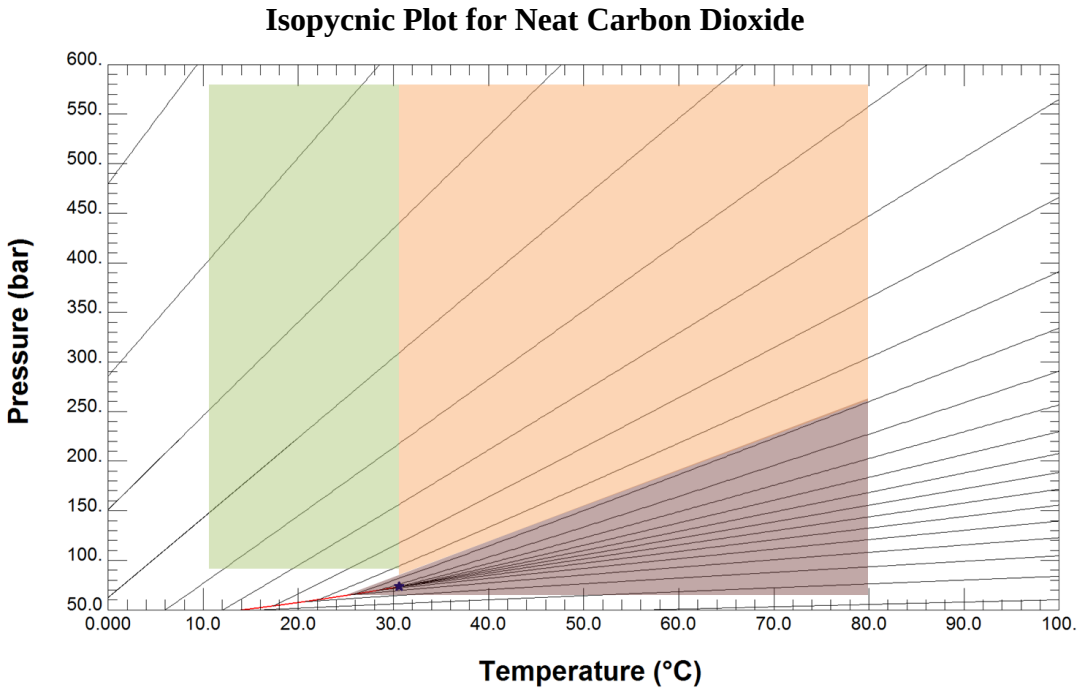

Figure 4. Perceived safe zones of operation in pSFC. The entire green region is sub-critical and considered safe for method development [5]. The Orange region is supercritical, with the same densities as the green region. It is also safe as long as the column stationary phase and analytes are stable at elevated temperatures. The red region is the compressible supercritical region, where efficiency losses are commonly observed [18]. Generated from REFPROP [1].

Figure 4. summarizes the current, somewhat arbitrary, safe zones of operation in SFC adapted from [5] and [18]. Current instrumentation is capable of operating at inlet pressures up to 600 bar and higher. The perceived lower limit for outlet pressure, to avoid compressibility effects, depends on the temperature and mobile phase composition, and the upper temperature limit depends on the analyte and column stability. The green region is sub-critical but above the critical pressure, and the orange region is supercritical. However, there are only slight differences between methods carried out in the green or orange region, along the constant density lines; the mobile phase is essentially a low viscosity liquid in both regions [5][9]. The red region, as you approach the gas phase above the critical temperature, has been-off limits due to poor efficiency caused by the compressibility of the mobile phase.

1.2.2 Efficiency and Plate Height in Uniform Colomns

Solute band dispersion works against band resolution in chromatographic systems, and minimizing the total band variance (σ^2) allows for better separations. The plate height (H) is a measure of the band variance per length (L) of column:

$$H = \frac{\sigma^2}{L} \tag{2}$$

Similarly, the separation power of a method is given by the total number of theoretical plates (N) and is equal to the column length divided by the plate height:

$$N = \frac{L}{H} \tag{3}$$

The number of theoretical plates can be easily calculated from the chromatogram using the following equation:

$$N = 5.54\left(\frac{t_r}{w_h}\right)^2 \tag{4}$$

where t_r is the retention time and w_h is the peak-width at half-height. The retention time is found in the normal way, subtracting the elution time for a retained solute from the time it takes an un-retained solute to traverse the column. Equation 4 is valid for Gaussian peaks and for distorted peaks is an overestimate of the true number of plates. It is acceptable for comparative purposes, though [23].

In uniform columns, where compressibility is not an issue, the plate height can be described as a function of the mobile phase linear velocity (u) by the classic vanDeemter equation:

$$H(u) = \frac{B}{u} + A + Cu \tag{5}$$

where A, B, and C are Eddy-diffusion, longitudinal diffusion, and resistance to mass transfer coefficients, respectively. In non-uniform columns, where compressibility issues arise, efficiency losses not described by Equation 5 can become significant and limit performance under certain conditions.

1.2.3 Excess Efficiency Loss in Non-Uniform Columns

Excess efficiency loss (decrease in N or increase in H) in the vicinity of the critical region has been a major topic of discussion in packed column SFC since it greatly limits the maximum speed and resolution predicted by the properties of the mobile phase and the vanDeemter equation. Early studies by Schoenmakers [13] attributed the excess efficiency loss to large pressure drops in columns packed with small particles, and they suggested that the use of small particles should be avoided in this region. This would be unfortunate since small particles are more efficient and have higher optimum linear velocities. Others concluded that broad distorted peaks under low density conditions resulted from a loss of analyte solubility in the mobile phase [14]. Recently, it has been shown that efficiency loss near the critical point is primarily the result of the formation of radial temperature gradients inside of the column [21]-[24]. Significant cooling can occur in SFC columns packed with small particles and operated at high flow rates as a result of isenthalpic expansion of the mobile phase[25]-[29][31][32]. This natural mobile phase cooling combined with heating the exterior wall of the column induces a radial temperature gradient along the column and radial distributions in important parameters such as mobile phase density (ρ) and velocity (u_m), and solute velocity (u_s) and retention factors (k). This process is summarized qualitatively in Figure 5.

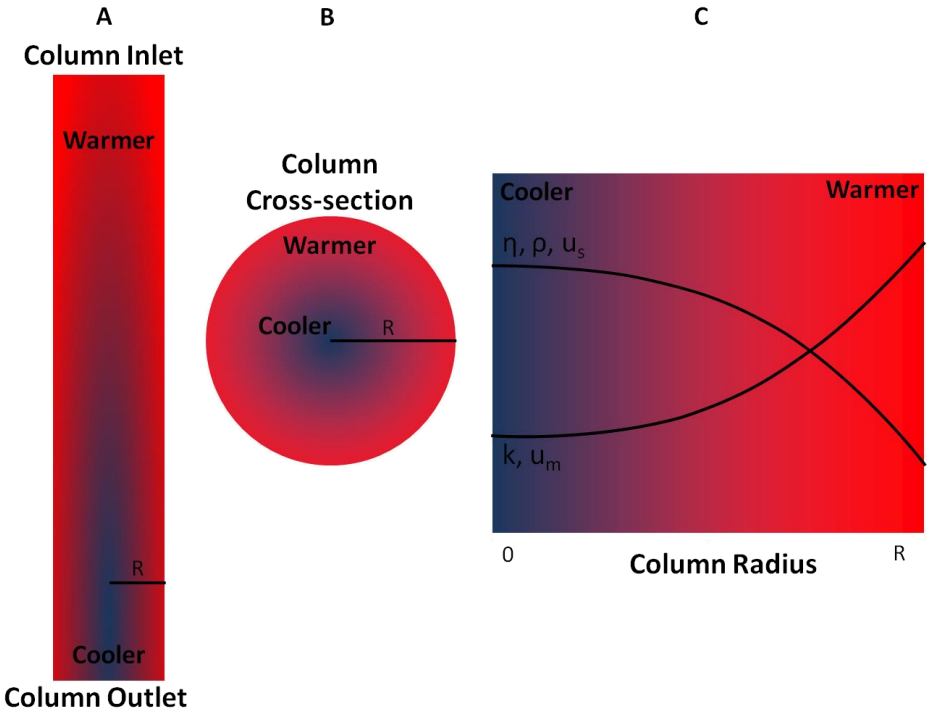

Figure 5. Radial Gradients in SFC. The red and blue colors correspond qualitatively to warmer and cooler areas inside of the SFC column. Diagram A shows the axial temperature gradients that result from the expansion of the mobile phase. Diagram B shows a cross-section of the radial temperature gradient, and diagram C shows how various mobile phase and solute parameters are affected by the radial temperature gradient. Legend: mobile phase viscosity (η), mobile phase density (ρ), Solute velocity (u_s), solute retention factor (k), mobile phase velocity (u_m)

Efficiency loss due to radial temperature gradients is not unique to SFC. It was first described as a result of viscous heating in HPLC by Poppe *et. al.*[30]. In SFC the situation is more complicated though, since the mobile phase is a compressible fluid. Flow through the column is generated by a pressure gradient from the inlet to the outlet of the column. In an adiabatic process, the temperature change can be calculated by solving equation (6):

$$\partial T = -\left(1-\alpha T\right)\frac{\partial P}{\rho C_p} \tag{6}$$

where α is the thermal expansion coefficient, and C_p is the isobaric heat capacity. Heating is observed in HPLC because the mobile phase is incompressible, the αT term is negligible and $-dP/\rho C_p$ is positive. In SFC, the αT term can be < 1, =1, or >1 depending on the temperature, pressure and mobile phase composition. As a result, only heating, heating and cooling, and only cooling are observed under different operating conditions

in SFC [31][32]. At low outlet pressures, the compressibility is high and the αT term always dominates and cooling is always observed. Rearranging equation (6) provides:

$$\partial T = -\left(\frac{1}{\rho C_p} - \frac{\alpha T}{\rho C_p} \right) \partial P \tag{7}$$

And the two terms in parentheses can be represented as a single coefficient called the Joule-Thomson coefficient (μ_{JT}):

$$\partial T = \mu_{JT} \partial P \tag{8}$$

This is convenient because if μ_{JT} is known for the mobile phase, the temperature drop that should accompany a given pressure drop can be predicted. In addition, if μ_{JT} is large problematic thermal effects might be expected. This provides valuable insight into temperature deviations and efficiency losses as you approach the critical point in SFC [33].

A simple method for predicting temperature drops in SFC columns has recently been developed using isenthalpic curves plotted on the P-T plane [29]. This method takes advantage of the fact that enthalpy (H) is a state function and that in an adiabatic process, such as JT cooling, the enthalpy change from the inlet to the outlet of the column will be equal to zero:

$$H_{in} = H_{out} \tag{9}$$

If the isenthalpic curves for the mobile phase are plotted on the P-T plane and the inlet temperature and pressure are measured, the isenthalpic line can be followed to the measured outlet pressure and the outlet temperature can be predicted graphically. Figure 6 summarizes this method for a column with an inlet temperature of 335K, outlet pressure of 150 bar, 100 bar pressure drop, and 5% methanol in CO_2 mobile phase. The black lines are the isenthalpic lines, and the red dashes are the JT coefficient (K/bar). This method can be carried out for any combination of inlet temperatures, outlet pressures and pressure drops as long as the equation of state for the mobile phase is known.

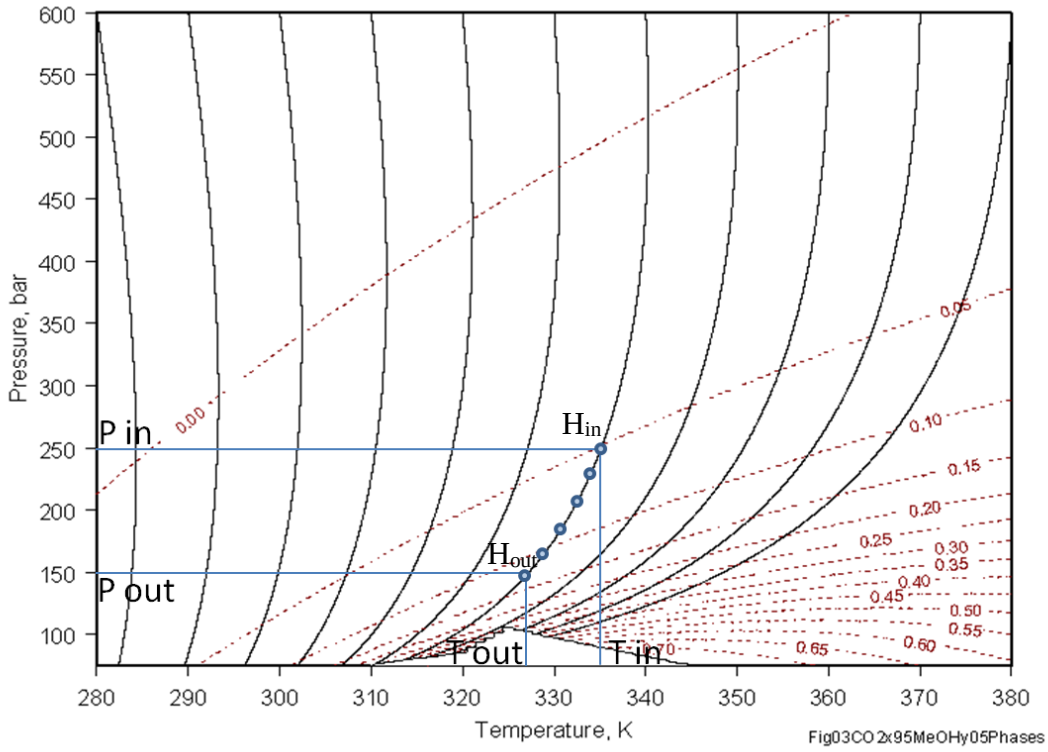

Figure 6. Representation of the isenthalpic method for estimating temperature drops in SFC columns [29]. The black lines are the isenthalpic lines, and the red dashes are the Joule-Thomson coefficient (K/Bar). The blue lines and dots represent hypothetical conditions for an adiabatic separation.

Since the excess efficiency loss described above is due primarily to a non-adiabatic transfer of heat from the column surroundings and the column center, improvements in HPLC [34][35] and SFC [21]-[24] have been observed by making the column more nearly adiabatic. This has involved using still air column heaters or thermal insulation. However, even in near-adiabatic columns, efficiency losses not described by Equation 5 still occur under low density conditions when the outlet pressure is decreased further [24].

1.3 Project Summary

This thesis project examines current limitations of operating in the supercritical region of the phase diagram, and it develops a method for expanding safe zones of operation to lower pressures near the critical point. A new technique of column thermostatting is presented that uses a specially designed column thermal environment

and the isenthalpic method described above. The goal is to operate the column adiabatically in order to eliminate the formation of radial temperature gradients and improve efficiency at low outlet pressures, where the mobile phase properties and solute retention are tunable with temperature and pressure.

2. Experimental Work

2.1 Equipment

2.1.1 Chromatography Equipment

All chromatograms were collected using a Hewlett-Packard Supercritical Fluid Chromatograph Model G1205A and a series 1050 HP diode array detector. The detector and reference wavelengths were set to 208 nm and 450 nm respectively, each with a bandwidth of 4 nm. Full loop injections were made using a Rheodyne 5092 injector with a 5-μL injection loop. The operating system was HP-SFC Chemstation Revision A.02.02 running under Microsoft Windows 3.1.

All connections from the injector to the column and from the column to the detector flow cell were made using 0.18-mm I.D. x 1/16" O.D. stainless steel tubing and Valco zero-dead-volume fittings. The length of tubing from the column outlet to the detector is approximately 45 cm, and from the injector to the column inlet is approximately 70 cm. A schematic of the entire chromatography system is shown below in Figure 7.

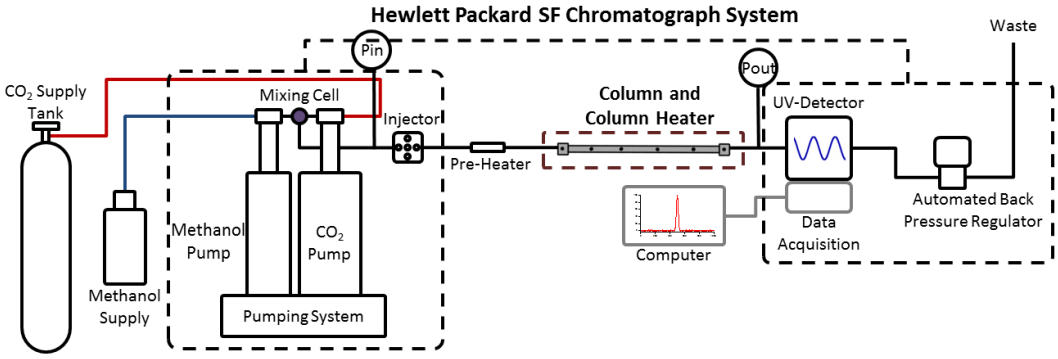

Figure 7. Overview of the supercritical fluid chromatograph used in this study.

2.1.2 Temperature and Pressure Measurements

The pressure and temperature at various points in the system were monitored to the nearest 0.1 bar and 0.1 K respectively, Figure 7 and Figure 8. The pressure transducers were Sensotec Model TJE or Model Super TJE and had a pressure range up to 600 bar. The TJE units were calibrated against the Super TJE unit to the nearest 0.1 bar over the pressure region of interest. The inlet pressure was monitored at a tee upstream from the injector, and the outlet pressure was monitored at a tee downstream from the column outlet. The extra-column pressure drop was corrected for by replacing the column with 20-cm of 0.76-mm I.D. x 1/16" O.D. SS tubing and inserting a third pressure transducer, Sensotec Model Super TJE, into the system at this point.

Small adhesive RTD probes were used to monitor the temperature of the outer surface of the column. The temperature of the mobile phase was monitored by placing an adhesive RTD probe on a union approximately 5 cm upstream from the column inlet. Four RTD probes were placed on the surface of the packed section of the column at positions x/L = 0.20, 0.40, 0.60, 0.80, where x is the distance from the column inlet (where the packed section begins) and L is the column length (250 mm), and on the column end fittings to monitor the temperature profile along the column. The RTD probes were connected to an Omega OM-CP-OCTRTD data logger and were calibrated to the nearest 0.1 K against a NIST-traceable digital thermometer (Fisher Scientific) accurate to ± 0.05 K.

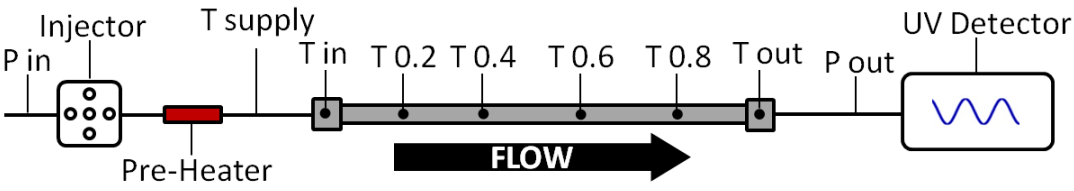

Figure 8. Location of the column temperature probes.

2.1.3 Columns

The columns used for all experiments described in this thesis were purchased from Phenomonex. Two different 250-mm x 4.6-mm I.D. columns packed with 5-μm particles were used, one with fully porous packing (Luna C18 2) and the other with superficially porous packing (Kinetex XB-C18).

2.1.4 Temperature Control

2.1.4.1 Mobile Phase Pre-Heater

A capillary heater (AgileSleeve model PTC050, from Analytical Sales and Products, Inc.) was inserted between the injector and the column to preheat the mobile phase to the desired inlet temperature. A 200-mm length of 0.18-mm i.d. x 1/16" o.d. stainless steel tubing was inserted into the capillary preheater. The mobile phase supply temperature was monitored using an adhesive temperature probe placed on a ZDV union approximately 5 cm upstream from the column inlet. The setting for the preheater was adjusted at each flow rate and pressure to yield an inlet temperature on the column end fitting that was equal to that of the target set temperature.

2.1.4.2 Column Thermal Environments

2.1.4.2.2 Commercial Still-Air Column Heater

A Brinkmann CH30 column heater was used for the commercial still air thermal environment. The column compartment dimensions (L x W x H) are 19.5 in x 2.75 in x 3 in. The heating source for this heater is mounted to the aluminum base plate of the column compartment. Temperature heterogeneity along the length of the column heater results in the inlet end being approximately 2 K warmer than the outlet end. Vertically, at the center of the column heater, the temperature near the base plate is approximately 3 K warmer than near the top of the column compartment. After up to 30 minutes of equilibration, temperatures inside of the column heater were steady to within 0.1 K.

2.1.4.2.3 Dual-Zone Still-Air Column Heater

The dual-zone still-air column heater was built in house and consisted of two heating zones that could be controlled independently using Omega CSC 32 PID controllers. The column heater was constructed using two 7.5-in long pieces of 1-in copper pipe. Each section was wrapped in resistive heating rope (Omega) and the two sections were connected using a copper pipe union. Once assembled, the total length of the column compartment was 16.5-in. The exterior surface of the unit was exposed to room air. Since each zone is controlled independently, the heater can be operated in both

isothermal and gradient heating modes. In isothermal mode the temperature distribution in the column heater is <±0.5 K from the inlet to the center to the outlet and up to ±25 K along the length in gradient mode. After up to 30 minutes of equilibration, temperatures inside of the column heater were steady to within 0.1 K.

2.2 Chemicals

Alkylbenzenes C10-C18(98.0% minimum purity) were purchased from Tokyo Chemical Industry Co. Methanol, acetonitrile, and methylene chloride were HPLC grade. LaserStar grade CO_2 (Praxair, 99.995% pure) was delivered from a supply tank with a dip tube.

2.3 Chromatography

All separations used a sample of either 1 mg/mL n-octadecylbenzene or a mixture of 0.5 mg/mL each of n-decylbenzene, n-dodecylbenzene, n-tetradecylbenzene, n-hexadecylbenzene and n-octadecylbenzene. All samples were prepared in a ternary mixture of equal parts acetonitrile, methylene chloride and methanol. Unless noted otherwise, all efficiency data was for octadecylbenzene. The mobile phase consisted of carbon dioxide with 5% methanol modifier (vol%). Under each set of conditions, three full-loop injections were made and the results averaged.

For all experiments, the inlet temperature was set such that the temperature of the inlet end fitting on the column agreed with the set temperature, within 0.1K. In adiabatic mode, the temperature at x/L=0.8 agreed with the predicted temperature ±0.2 K under most conditions. A wide range of temperatures and pressures from 40^{o}C to 60^{o}C and from 75 bar to 240 bar were employed, and van Deemter curves were generated under selected conditions using various thermal modes. In adiabatic mode, zone 2 of the heater had to be adjusted at each flow rate and pressure as the predicted temperature profile changed.

2.4 Related Work

In related work performed in this laboratory, additional separations of the alkylbenzene mixtures were performed using the same columns operated in a forced-air thermal environment. This set up is described in detail in reference [33]. For this study, the column was suspended in a forced-air (GC-type) oven, and temperatures and pressures were monitored as described in Figure 8.

3. Results and Discussion

3.1 Design and Implementation of the Dual Zone Tube Heater

Under typical operating conditions in SFC, the Joule-Thomson coefficient (μ_{JT}) is positive and cooling is observed from the inlet to the outlet of the column. At low outlet pressures above the critical temperature, μ_{JT} is larger and more cooling occurs. Under these conditions, for a particular column and solute system, radial gradients in solute velocity cause increased band spreading for various combinations of temperatures and pressures. It has been shown that radial solute velocity gradients are due primarily to the formation of radial temperature gradients, and that minimizing radial temperature gradients improves efficiency up to a certain point. This has been demonstrated by observing changes in efficiency for columns operated in forced-air and in still-air environments, and in insulated columns. An alternative method for column thermostatting is developed and presented here and compared to results obtained in forced-air and still-air. The new dual-zone column heater described herein, also referred to as the tube heater or gradient heater, is designed to provide a radially uniform thermal environment that closely matches the natural axial temperature profile of the mobile phase along the column. This design is intended to provide a near-ideal adiabatic system that further reduces the magnitude of the radial temperature gradients that form in packed columns and improve efficiency over a wider range of temperatures and pressures.

In order for a column to operate adiabatically, the temperature along the column wall from the inlet to the outlet needs to match the temperature of the fluid inside the column. Under this condition, there will be no heat transport across the column wall

between the external environment and the fluid inside the column. Current column heater designs are inherently flawed in this regard, since they offer only one heating zone. This means the temperature is set at a single value, and the entire thermal environment is heated to the set value. In a forced-air oven, significant heating occurs along the column since there is efficient heat transport between the circulating hot air and column surface. The column end fittings, due to their larger size and surface area, are heated more efficiently than the main column itself. A schematic of this thermal mode is presented in Figure 9. This method of column thermostatting is non-adiabatic.

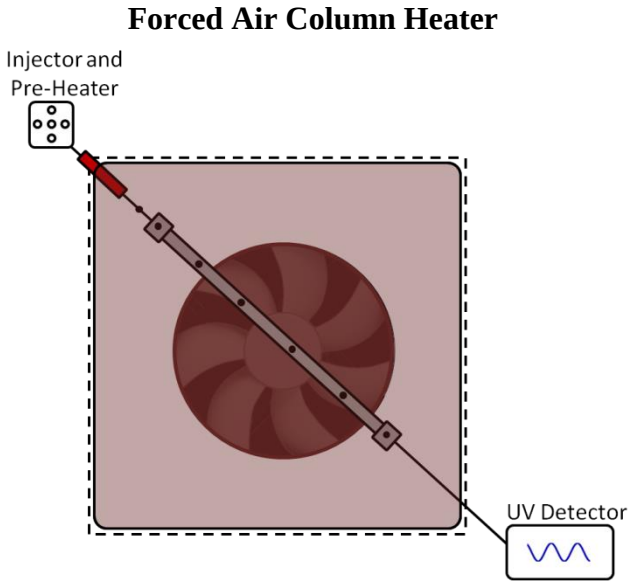

Figure 9. Column placement in the forced-air setup.

While less prominent, a similar situation occurs in commercially available still-air column heaters. The major difference between the forced-air and still-air thermal environments is the efficiency of heat transport from the surrounding air to the column wall. Still air is much less efficient at heating the column wall and as a result the column is allowed to cool more; less heating occurs near the outlet. However, some heating does still occur since the temperature of the surrounding air is higher than that of the column outlet. A schematic of this thermal mode is presented in Figure 10. This method of column thermostatting is near-adiabatic.

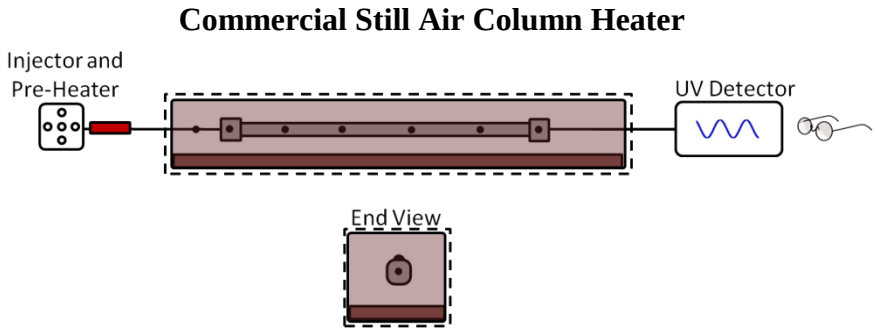

Figure 10. Column placement in the commercial still-air setup.

Li and Thurbide [36] were able to improve column efficiency under low density conditions by locally heating the inlet or locally cooling the outlet of the column. The improvement was attributed to "changing the local fluid density within the affected column region", by observing changes in relative retention times; retention times increased when heating the inlet and decreased when cooling the outlet. At the time, the general consensus was that the density drop along the column resulted in efficiency loss. In section 1.2.3 recent work is introduced which suggests this efficiency loss is due to the radial temperature gradients that result from a thermal mismatch between the column wall and the mobile phase. With this in mind, another explanation for the results observed by Li and Thurbide is that by heating the inlet or cooling the outlet, they have imposed a temperature gradient along the column that offsets the effects of the cooling mobile phase and reduced the magnitude of the radial temperature gradient near the outlet. A full discussion of the temperature drop and pressure drop was not provided in their work, however. They did note that when heating the column inlet too little only modest improvements were made and too much heating resulted in poor peak shapes again. This suggests that there is an optimum axial column temperature gradient that minimizes efficiency loss under low density conditions.

The dual-zone tube heater provides a near-ideal adiabatic environment that is designed to remove the radial temperature gradients that form in traditional column thermostatting modes. It was designed to specifically address two major flaws in current still-air column heaters. First, since efficiency loss is primarily due to radial thermal heterogeneity under conditions where μ_{JT} is large, the thermal environment for packed column SFC should be as radially homogeneous as possible. Second, the outlet end needs to be controlled separately from the inlet end in order to account for the cooling that occurs along SFC columns and avoid imposing radial temperature gradients near the outlet of the column. Given the results by Thurbide and our understanding of what controls efficiency loss at low outlet pressures, we set out to try to develop a thermal environment that allowed us to precisely control the temperature gradient along the column. Initial efforts were made to actively cool the column outlet using PID-controlled thermoelectric devices attached to the column. Using TEDs presented some practical challenges based on the amount of hardware required and in our tests did not provide uniform cooling at the outlet. Multiple TEDs would need to be attached and function in unison in order to uniformly remove heat from the surface of the column. TEDs also require the use of a bulky heat sink. All of the hardware required complicated the design and use of this method and decreased the robustness of this approach.

Another design attempted to directly heat the inlet and outlet of the column using PID-controlled resistive heating tape, while insulating or gently heating the rest of the column. This approach was attractive due the rapid thermal equilibration and dynamic temperature control provided by directly heating the column surface. Less hardware was required since the need to cool the column with TEDs was no longer necessary. The most effective iteration of this design used three heating zones. The inlet and outlet end fittings of the column were heated directly using specially designed resistive heating elements that slid onto the ends of the column. The middle section of the column was gently heated by a copper pipe that was wrapped in resistive heating rope. While this design was promising, we were unable to keep the column temperature from oscillating as a result of the PID feedback controllers that were thermostatting the column end fittings. We

concluded that direct on-column heating or cooling was too difficult to achieve the degree of thermal control we desired, ±0.1K. A photo of this setup is shown below.

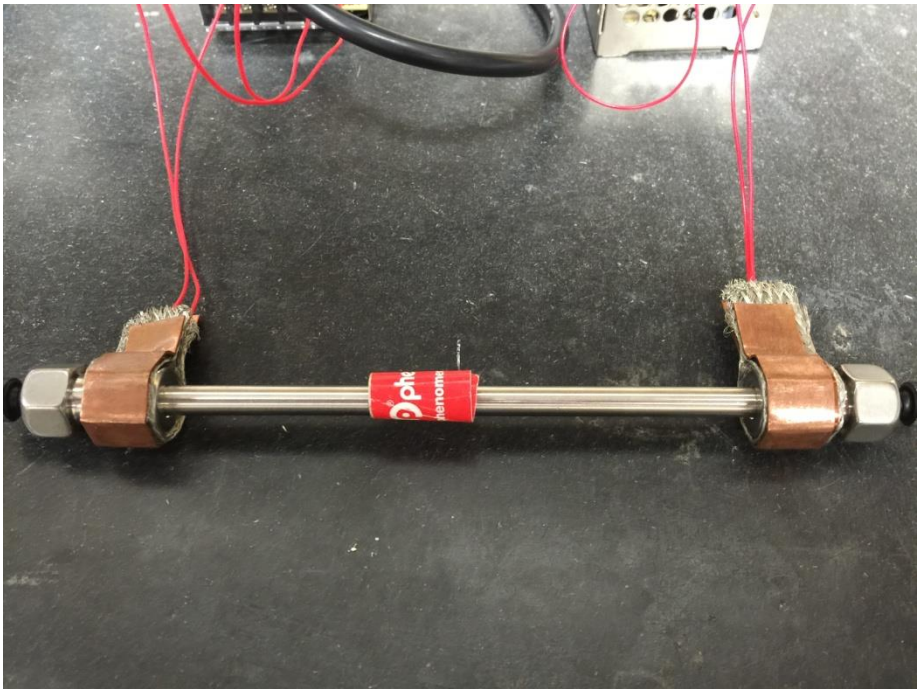

Figure 11. Direct on-column temperature control. The third heating zone was removed to show the on-column heating elements.

We settled on using a simple two-zone still-air set up, with the column suspended inside the thermal environment. Without direct on-column control or a fan circulating hot air, the still-air approach suffers from extended equilibration times up to 30 minutes. The advantage is that oscillations due to the feedback controllers do not affect the on-column temperature in a noticeable way since air is insulating the column from the heating source. The end result is a very stable temperature after equilibration, ±0.1K. The column was suspended inside two sections of 1-inch diameter copper tube each wrapped in resistive heating rope and controlled using PID controllers. The inlet, zone 1, could be controlled independently of the outlet, zone 2. The two zones were connected using a copper union in order to obtain a smooth temperature transition from zone 1 to zone 2. Copper tubing was selected to house the column because it is radially homogeneous and able to accommodate columns of different dimensions. This system is more robust than the previous designs since the temperature is relatively easy to control, the design is simple and free of excessive hardware, and no custom column-specific heating elements

are required. The result is a simple theromstatted device that offers the flexibility to operate the column in an isothermal still-air environment, or in a thermal gradient still-air mode which more closely matches the natural temperature profile of the mobile phase. This design is shown in Figure 12 and Figure 13.

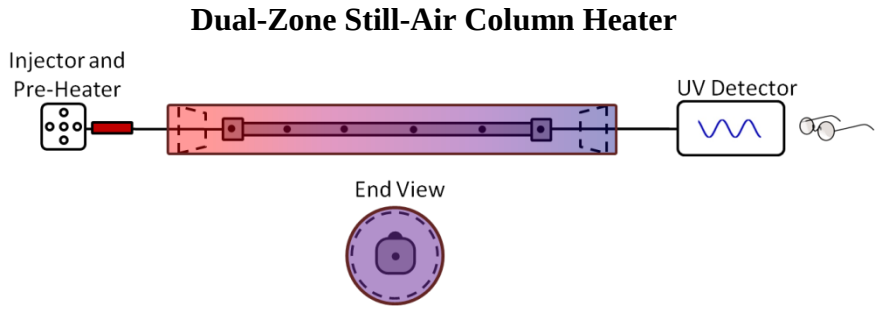

Figure 12. Column placement in the dual-zone tube heater. Red and blue correspond to warmer and cooler regions in the tube heater.

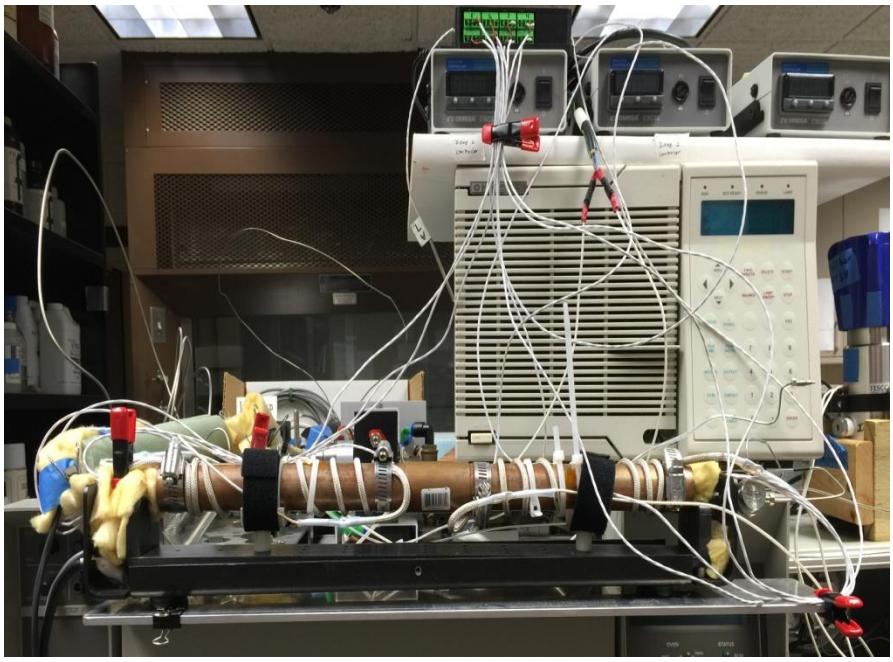

Figure 13. Photo of the dual-zone still-air column heater that was designed to operate the column adiabatically. On the left is "zone 1" which is controlled by the PID controller on the top left, and on the right is "zone 2" which is controlled by the PID controller on the top right.

Figure 14 shows the measured temperature profile along the surface of the column as a function of time, for the tube heater operating in adiabatic mode. The temperature data corresponds to the measured on-column temperature with flow and with no flow. After performing a series of injections, flow was stopped in order to check the temperature distribution of the tube heater. The temperature profile of the thermal

environment (temperature measurements with no flow) matched the column temperature profile with flow within 0.5°C at all points along the column. If the column was perfectly adiabatic, the flow and no-flow temperature profiles would be exactly the same. This was never the case since there is not only cooling occurring along the column from the mobile phase, but also conduction along the stainless steel column wall. In adiabatic mode, the temperature distribution of the tube heater was checked using this flow/no flow check procedure throughout the early experiments to ensure that the heater was performing predictably. If there was a temperature mismatch, the heater could be adjusted so that the column temperature profile with no flow agreed with the column temperature profile with flow before continuing. This greatly increased the time required to collect data however, since it takes time for the column to equilibrate once flow is started and is not feasible for routine implementation.

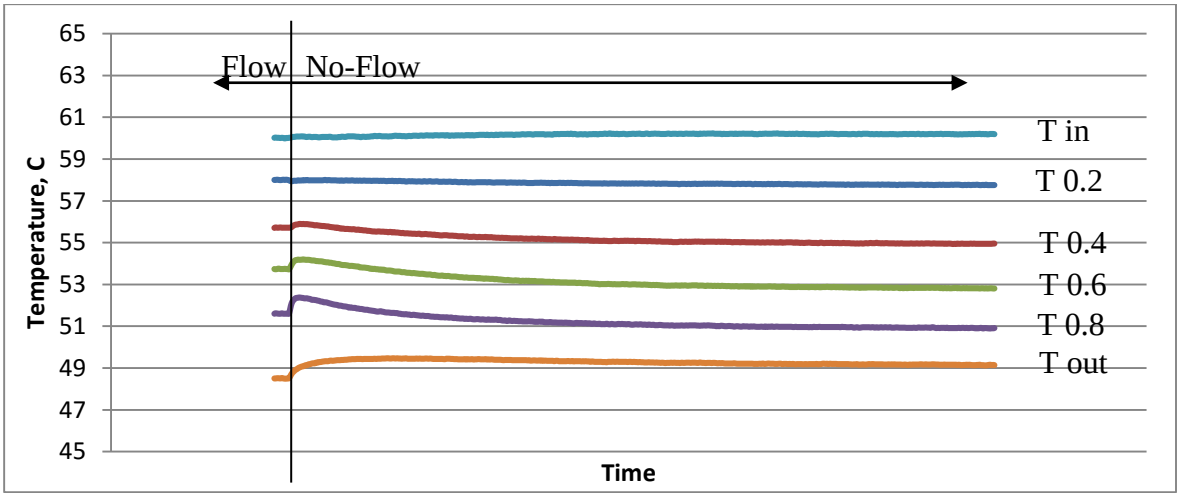

Figure 14. Flow to no flow check procedure used to determine if the thermal environment was matching the adiabatic profile of the column. With no flow, the temperature distribution of the thermal environment should match the column temperature profile with flow, if the system is adiabatic. Heat conduction along the column makes this difficult in practice. Conditions: Kinetex Column, 3mL/min, 60°C inlet temperature, 90 bar outlet, μ_{JT}≈0.8 K/bar. These represent some of the most challenging conditions used in this study.

Normal operation of the tube heater required setting the temperature of the heater with no flow before starting the experiment so that the column inlet matched the target operating temperature. Once this was set, flow was started and the supply temperature was adjusted so that the inlet temperature agreed with the target temperature again. Once the inlet and supply temperature were set, the enthalpy was calculated using an Excel program running REFPROP 9.0 [1] and based on the method outlined in section 1.2.3,

using the measured inlet temperature and the corrected column inlet pressure. The predicted outlet temperature was calculated from the corrected column outlet pressure assuming isenthalpic expansion. After the outlet temperature was calculated, zone 2 of the tube heater was adjusted so that the measured column temperature profile agreed with the calculated adiabatic temperature profile. To change operating conditions at the same inlet temperature, the new conditions were set and the supply temperature was changed so that the inlet temperature agreed with the target temperature. A new outlet temperature was calculated and zone 2 was adjusted so the on-column temperature agreed with the calculated temperature. In order to change the target inlet temperature, it was necessary to stop the experiment and reset the thermal environment for the new target temperature. For routine application, the flow/no flow check procedure described in the previous paragraph was not used to determine if the column was operating adiabatically.

To determine if the column was operating adiabatically, the on-column temperature profile was compared to the predicted fluid temperature profile. To simplify the method even further, the last temperature probe on the packed section of the column (x/L=0.8) was used to set the thermal environment in adiabatic mode. This provided a simple set point for determining the set temperatures for the heater and evaluating whether or not the column was operating adiabatically. The probe at x/L=1.0, which corresponds to the outlet of the column, was attached to the bulky column end fitting and under some conditions responded inconsistently; this was particularly true at low outlet pressures. Representative column temperature profiles for three different thermal environments, each for the same set operating conditions (oven or inlet temperature, outlet pressure, flow rate), are shown in Figure 15. The measured on-column temperature profiles (dots) are compared to the predicted adiabatic temperature profiles (solid lines) for the Kinetex column operating in each thermal environment for the same set conditions. For the column in forced air, the difference between the predicted outlet temperature (solid lines) and the measure outlet temperature (dots) in is greater than 3.0 K. In still air, this difference is 1.0 K, and in adiabatic mode this difference is 0.1 K. This trend in temperature profiles is consistent for all experiments where significant cooling

occurs; forced-air is “non-adiabatic”, still-air is “near-adiabatic” and the tube-heater in adiabatic mode in “near-ideal adiabatic”.

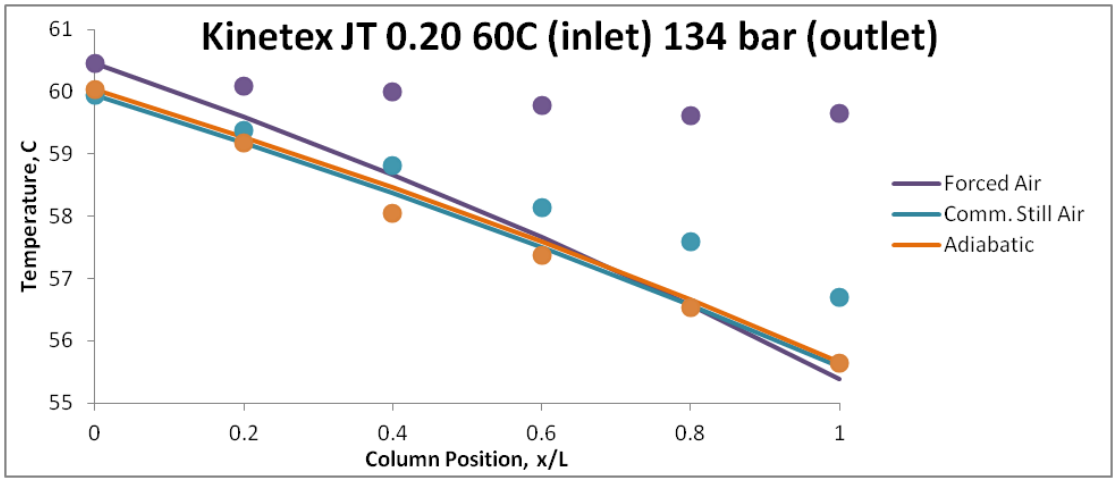

Figure 15. Measured column temperature profile (dots) compared to the adiabatic, or isenthalpic temperature profile (lines) for three different thermal environments.

Even if the on-column temperature profile matched the adiabatic temperature profile of the mobile phase perfectly, the actual temperature profile inside the column is going to be somewhat different and radial temperature gradients will still be present. There are complex heat transfer processes that occur inside and along the column that cannot be predicted without the benefit of advanced numerical modeling. A major problem arises from the fact that the column is stainless steel with large end fittings and a fixed thermal conductivity that is much higher than that of the packed bed. The packing material is partially porous and non-porous functionalized silica, and the thermal conductivity of the mobile phase changes along the entire length of the column. These mismatches in the thermal conductivities means that, without efficient, direct on-column control of the temperature profile along the column wall, its temperature profile will not in general match that of the packed bed. This is partly why considerable effort was made initially to actively heat/cool the column directly. This would allow fast thermal equilibration and precise control of the temperature profile along the column. Instead, we are trying to minimize heat transport across the column wall and allow the mobile phase to control the column temperature. We termed this method of heating the column as “soft

heating". All radial temperature gradients cannot be removed by only taking into account the mobile phase properties because there are numerous other parameters contributing to the actual temperature of the mobile phase inside the column.

3.2 Effect of the Thermal Environment on Chromatographic Performance

3.2.1 Performance of the Kinetex Column in a Forced-Air Oven

A previous related study in our lab [33] was conducted using the same 250mm x 4.6mm x 5um Kinetex and Luna columns in a forced-air thermal mode. In that study, the efficiency of n-octadecylbenzene was measured at 3mL/min for operating temperatures from 20-80 ^{o}C and for outlet pressures from 90-250 bar for CO_2 mobile phases containing 5, 10, and 20% methanol. Excess efficiency loss was found to occur along JT isopleths, over a wide range of operating conditions for a given column. The data collected in the forced-air study was used throughout this thesis for comparison with data collected in still air and gradient thermal modes for the same columns.

3.2.2 Performance of the Kinetex Column in a Commercial Still-Air Column Heater

In the current study, the Kinetex column was operated in the commercial still air (near-adiabatic) heater. These two thermal environments, forced-air and still-air, represent the most common column thermostatting techniques for packed column SFC. First, the low pressure performance limits for the commercially available still-air column heater were compared to those obtained in forced-air for the Kinetex column, over a range of temperatures from 40-60 ^{o}C. An optimum flow rate was chosen for the conditions of interest from the van Deemter plots in Figure 16. At 50^{o}C, the optimum flow rate was between 2 mL/min and 3 mL/min over a wide range of pressures. A flow rate of 3 mL/min was chosen as the optimum flow rate for the Kinetex column, and this flow rate was used to study the effect of outlet pressure on efficiency for the different thermal environments. Overall, the lower pressure limit is decreased drastically for columns that are operated in still-air mode compared to forced-air mode. This is shown in

Figure 17, where the reduced plate height begins to increase as the outlet pressure is decreased. The results for this Kinetex column are consistent with previous observations for different columns going from forced air to thermally insulated columns and columns in still air.

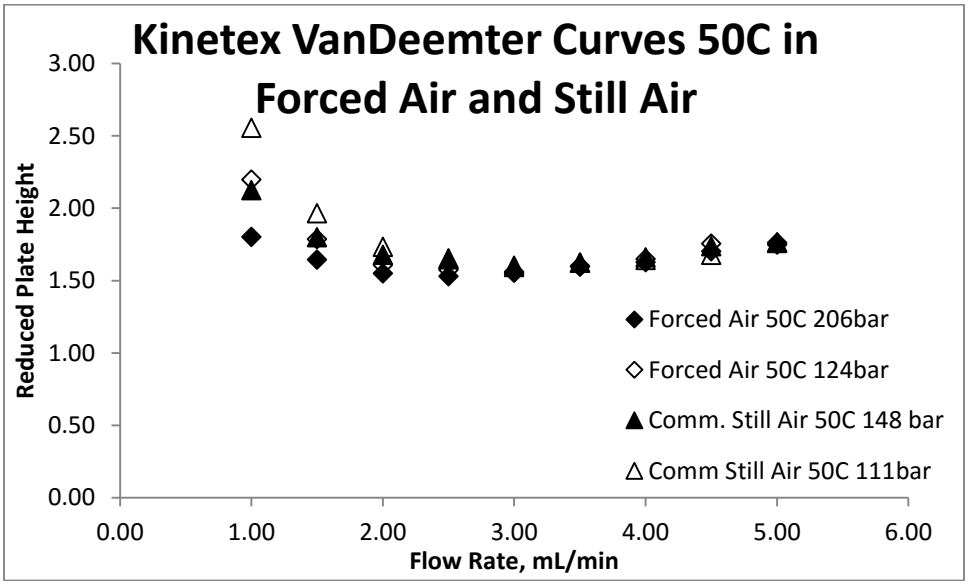

Figure 16. Van Deemter curves generated in still air and compared to previous van Deemter curves in forced air under uniform conditions for the Kinetex column.

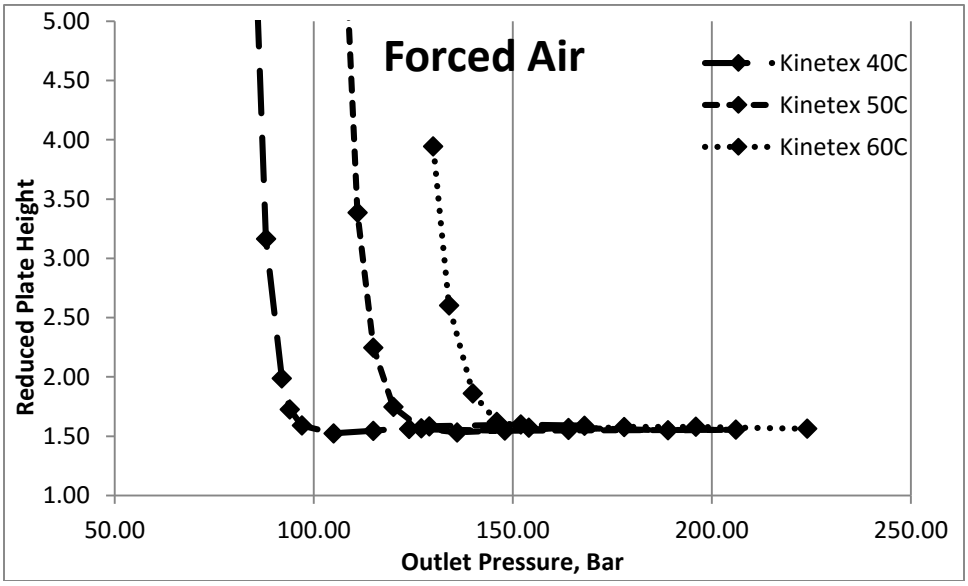

Figure 17. Effect of outlet pressure on efficiency in forced-air [33]. At 40, 50, and 60 ^{o}C efficiency starts to degrade at 92, 115, and 136 bar respectively.

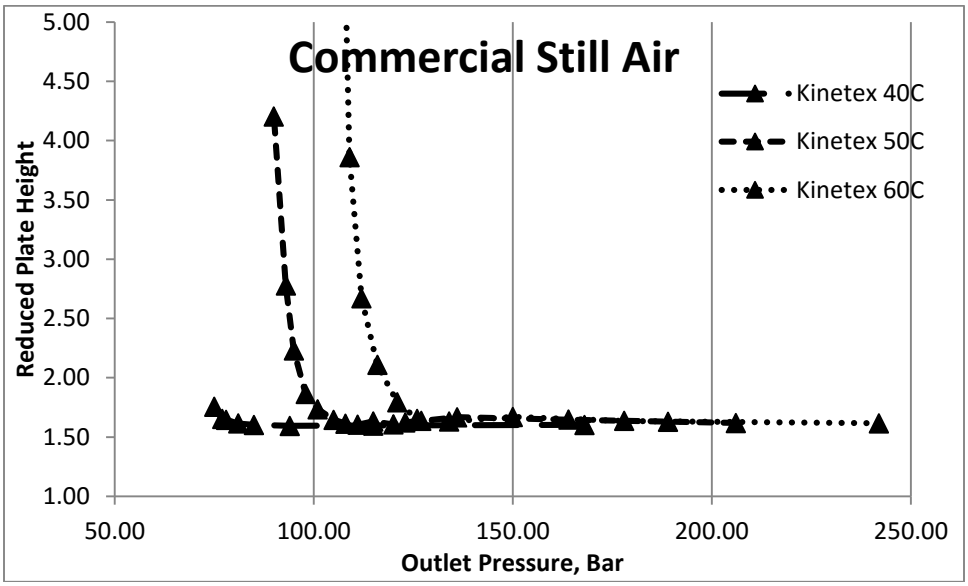

Figure 18. Effect of outlet pressure on efficiency in still-air. At 50, and 60 °C efficiency starts to degrade at 98, and 116 bar respectively. At 40 °C very little efficiency loss is observed before out-gassing occurs at the detector.

In forced air, efficiency loss (>25% increase in the reduced plate height relative to the average obtained at higher outlet pressures) began to occur at outlet pressures of 92 bar, 115 bar, and 136 bar at 40, 50, and 60°C respectively. For the Kinetex column, the average plate height under uniform conditions was 1.6, so a 25% increase in the plate height corresponds to a value of 2.0 particle diameters. In commercial still air, efficiency loss occurred at an outlet pressure of 96 bar, 101 bar, and 116 bar at 50, and 60°C respectively. A greater than 25% increase in the plate height was never observed at 40 °C. This improvement in performance has been attributed primarily to a decrease in heat transfer from the column wall towards the center of the column thus decreasing the magnitude of the radial temperature gradients that form inside of the column. It follows then that further decreasing the magnitude of the radial temperature gradients will lead to further improvements in chromatographic performance at even lower outlet pressures at 50 and 60 °C.

3.2.3 Performance of the Kinetex Column in the Dual-Zone Still-Air Column Heater

The dual-zone column heater was designed to provide a near-ideal adiabatic thermal environment. The temperature profile inside of the column heater can be varied from isothermal, similar to the commercially available still air heater, to a maximum

gradient of about 25 K from column inlet to column outlet. The dual-zone column heater was operated in isothermal mode and the efficiency results were compared to those obtained with the commercially available still air heater in Figure 19 below. There is essentially no difference in the two plots of efficiency versus outlet pressure for the commercial still air heater and the dual-zone heater operated in isothermal mode.

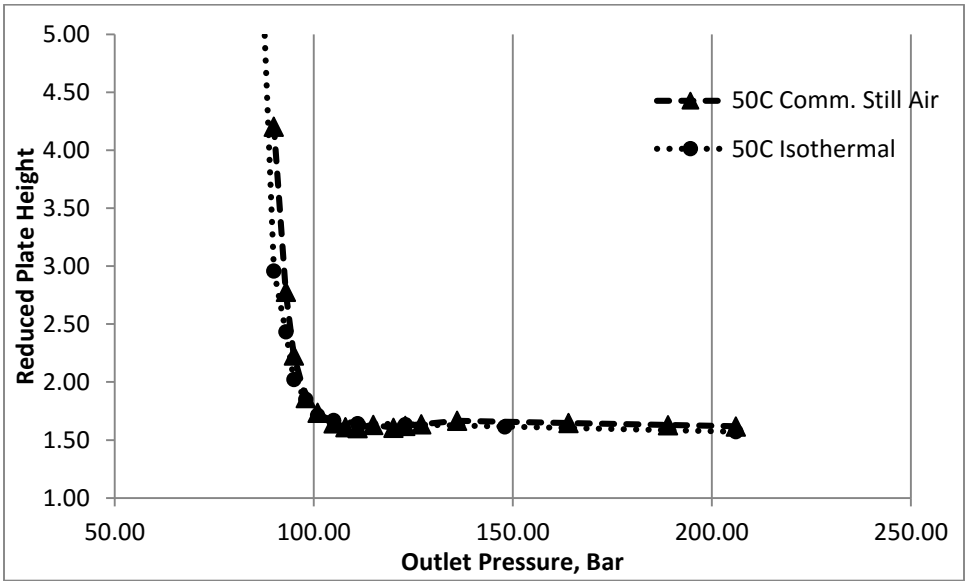

Figure 19. Comparison of the tube heater operating isothermally, to the commercially available still-air column heater.

The same experiment was repeated with the thermal environment operating in two different temperature gradient modes and compared to the isothermal mode in Figure 19. First, a constant 6 ^{o}C temperature gradient along the axis was used. Second, the column was operated adiabatically. In gradient mode the inlet end, zone 1, of the column heater is set such that the on column temperature at the inlet of the column is warmer than the outlet. In this case the inlet was set to 50^{o}C (the set operating temperature) and the outlet was set to 44^{o}C. This change in the thermal mode, imposing a 6^{o}C temperature gradient, caused an 8-bar decrease in the minimum outlet pressure that could be used with no excess efficiency loss. This lowered the minimum outlet pressure from ≈95 bar to ≈87 bar and caused the apparent retention factor for octadecylbenzene to increase from 6.61 to 9.26.

Using the isenthalpic method previously described, the thermal environment was adjusted so that the temperature profile along the column wall closely matches the predicted temperature of the mobile phase. In order to operate the column heater in adiabatic mode, the predicted column outlet temperature was calculated based on the inlet operating temperature, column inlet pressure, column outlet pressure and the equation of state for the fluid. The necessary calculations were done using REFPROP 9.0 [1]. In this mode, the measured outlet temperature typically agreed with the predicted temperature within 0.2 ^{o}C under most conditions. Operating adiabatically further decreased the minimum outlet pressure to ≈82 bar, which increased the retention factor for octadecylbenzene to 17.23 with no excess efficiency loss.

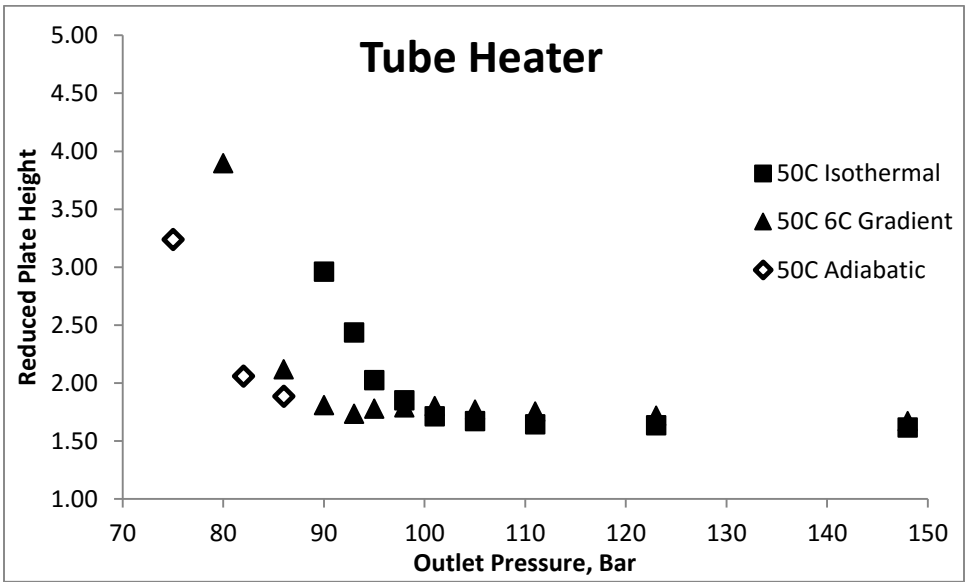

Figure 20. Tube heater operating in isothermal mode (squares) gradient mode (triangles) and adiabatic mode (open-diamond).

3.2.4 Summary of the Kinetex Column Performance in Different Thermal Environments

Figure 21 and Figure 22 compare the efficiency data at 50^{o}C and 60^{o}C as a function of the outlet pressure, for all three thermal environments (forced-air, still-air, and adiabatic). Performance at low outlet pressures is influenced greatly by the column thermal environment, and performance can be improved substantially by minimizing the formation of radial temperature gradients, by operating the column nearly adiabatic. This

was previously shown going from forced-air to still-air [21]-[24], and is true for this Kinetex column as well. Efficiency is further improved at lower outlet pressures by matching the column surface temperature to the predicted temperature of the fluid inside of the column. Efficiency loss does still occur in adiabatic mode; however it occurs at lower outlet pressures compared to isothermal heating modes at the same temperature.

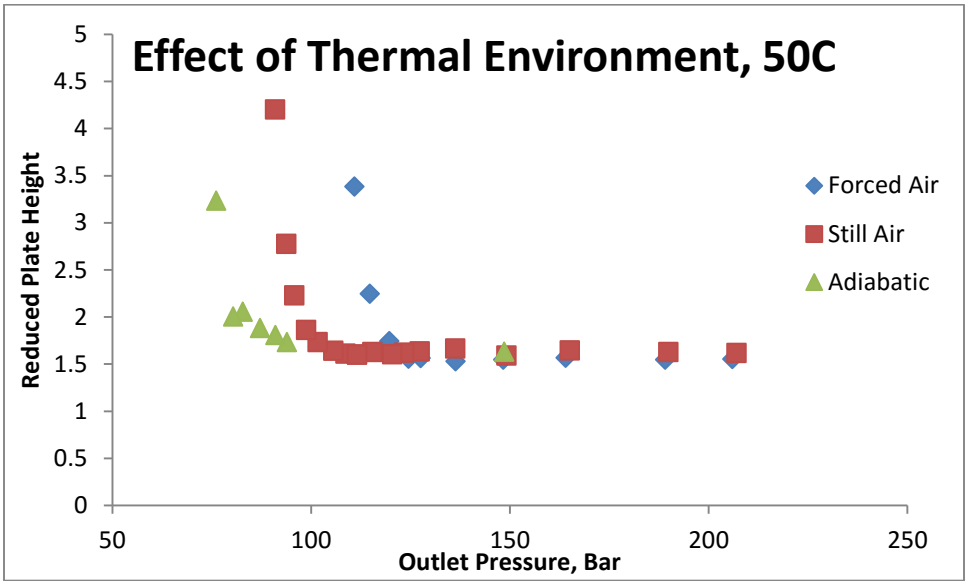

Figure 21. Effect of the thermal environment on efficiency at 50 °C for the Kinetex column.

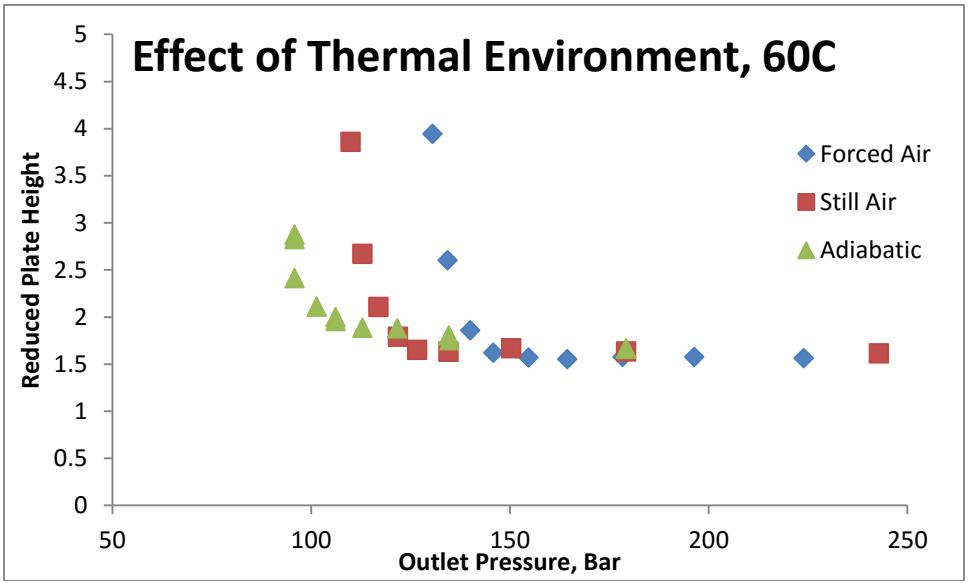

Figure 22. Effect of the thermal environment on efficiency at 60 °C for the Kinetex column.

The onset of excess efficiency loss was observed at a different outlet pressure for each temperature that was studied in a given thermal environment. This makes it difficult to predict when efficiency losses will occur. Efficiency maps attempt to relate the observed efficiency loss to the thermophysical properties of the mobile phase. Previous attempts to map efficiency losses were made by Tarafder and Guiochon [5]. They observed that efficiency loss occurs where the isopycnic lines are closely spaced. Similarly, the efficiency maps presented below relate the efficiency loss observed for octadecylbenzene to the Joule-Thomson coefficient of the mobile phase. Since the efficiency loss is due primarily to radial thermal heterogeneity, the extent of cooling that occurs is an important factor in determining efficient operating conditions. The Joule-Thomson coefficient (8) has units of K/bar and provides a measure of the temperature drop that accompanies a given pressure drop. Even though μ_{JT} is changing along the entire length of the column a formal coefficient that is representative of the general operating conditions can be defined based on the inlet temperature and outlet pressure [33]. This value is an overestimate of the actual μ_{JT} but it is simple to calculate from the experimental setup.

The formal JT coefficient predicts efficiency loss for columns operated in a given thermal environment at different temperatures. For a given column, solute and thermal mode, excess efficiency loss from 40^{o}C to 60^{o}C is relatively constant along JT isopleths [33]. For the Kinetex column in forced air, the plate height begins to increase at a JT coefficient of 0.15 K/bar [33]. In commercial (isothermal) still air, efficiency loss occurs at a JT coefficient of 0.20 K/bar and increases sharply for larger JT coefficients (Figure 24). In adiabatic mode, some efficiency loss occurs again at a JT coefficient of 0.20 K/bar however, the increase in the plate height is much less rapid for larger JT coefficients (<25% increase in h up to a JT coefficient of 0.50K/bar); the plate height increased rapidly for JT-values greater than 0.5 K/bar at 60 ^{o}C. Operating the column adiabatically can tolerate more challenging mobile phase conditions before drastic increases in the plate height are observed.

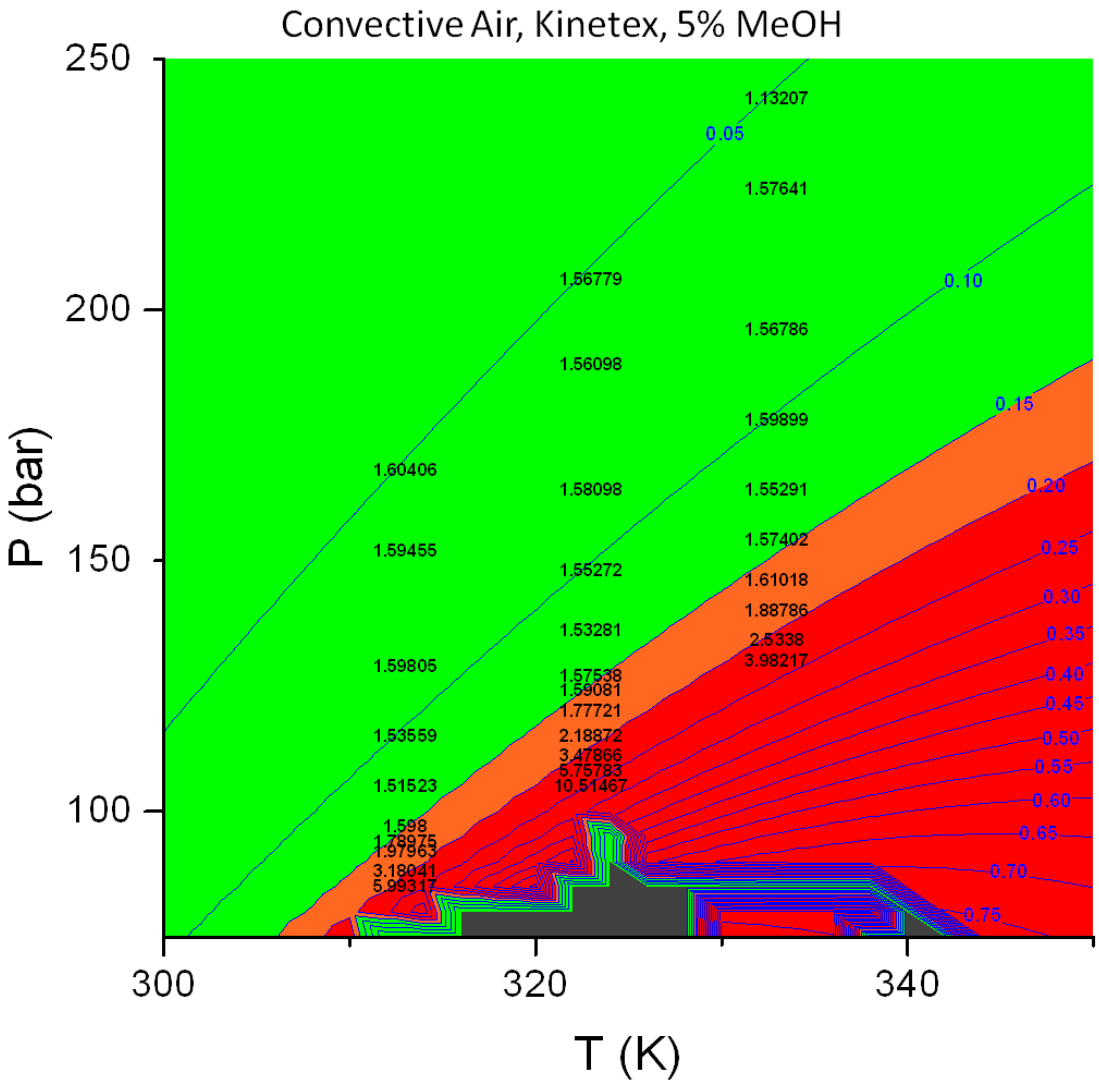

Figure 23. Efficiency for octadecylbenzene on the Kinetex column in forced-air thermal mode. The blue contours are the Joule Thomson coefficient (K/bar), and the black numbers are the apparent plate height at the corresponding temperature and pressure. The green region represents no efficiency loss, the orange region represents moderate efficiency loss (<25%) and the red region represents excess efficiency loss (>25%).

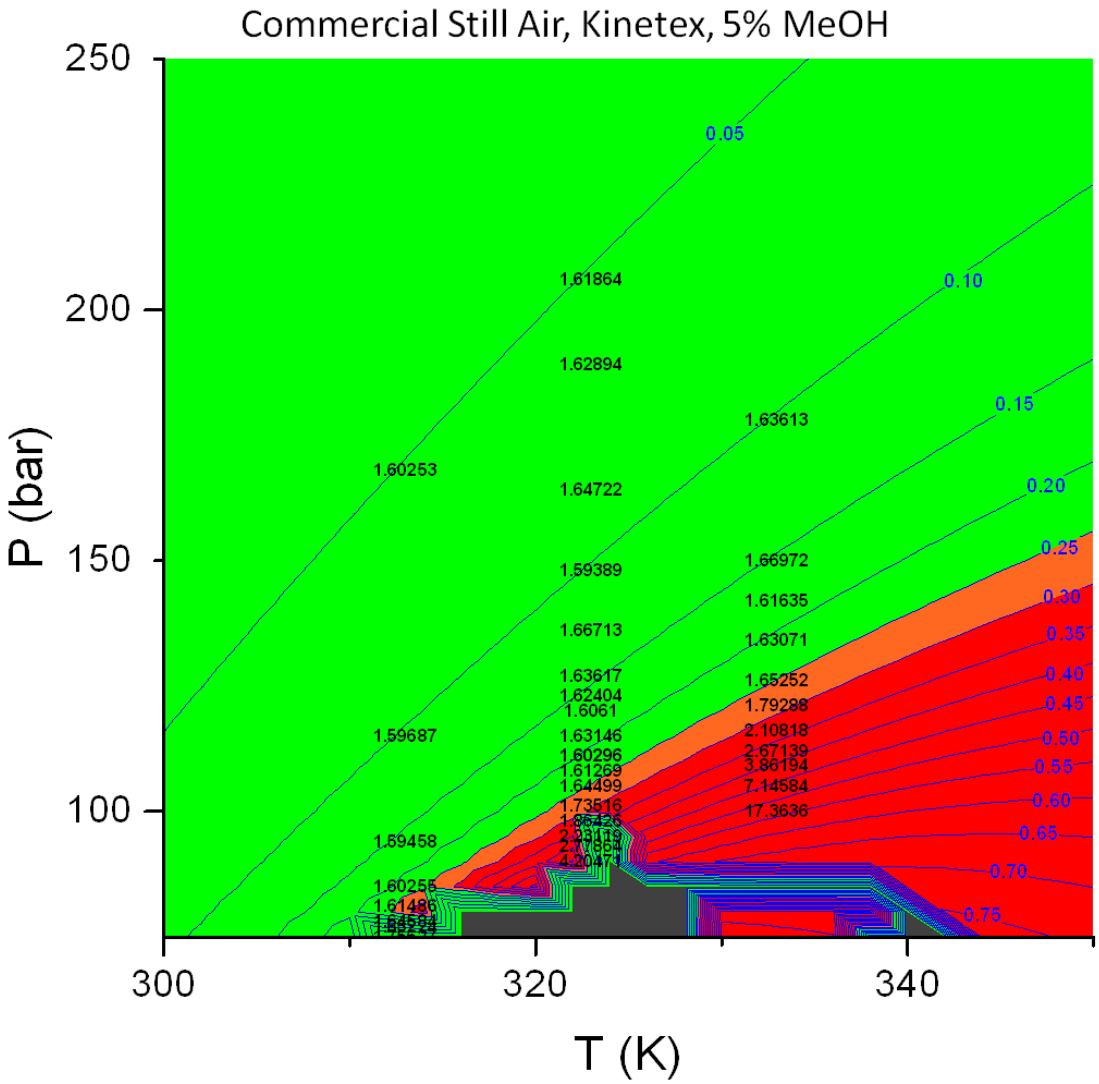

Figure 24. Efficiency for octadecylbenzene on the Kinetex column in isothermal still-air mode. The blue contours are the Joule Thomson coefficient (K/bar), and the black numbers are the apparent plate height at the corresponding temperature and pressure. The green region represents no efficiency loss, the orange region represents moderate efficiency loss (<25%) and the red region represents excess efficiency loss (>25%).

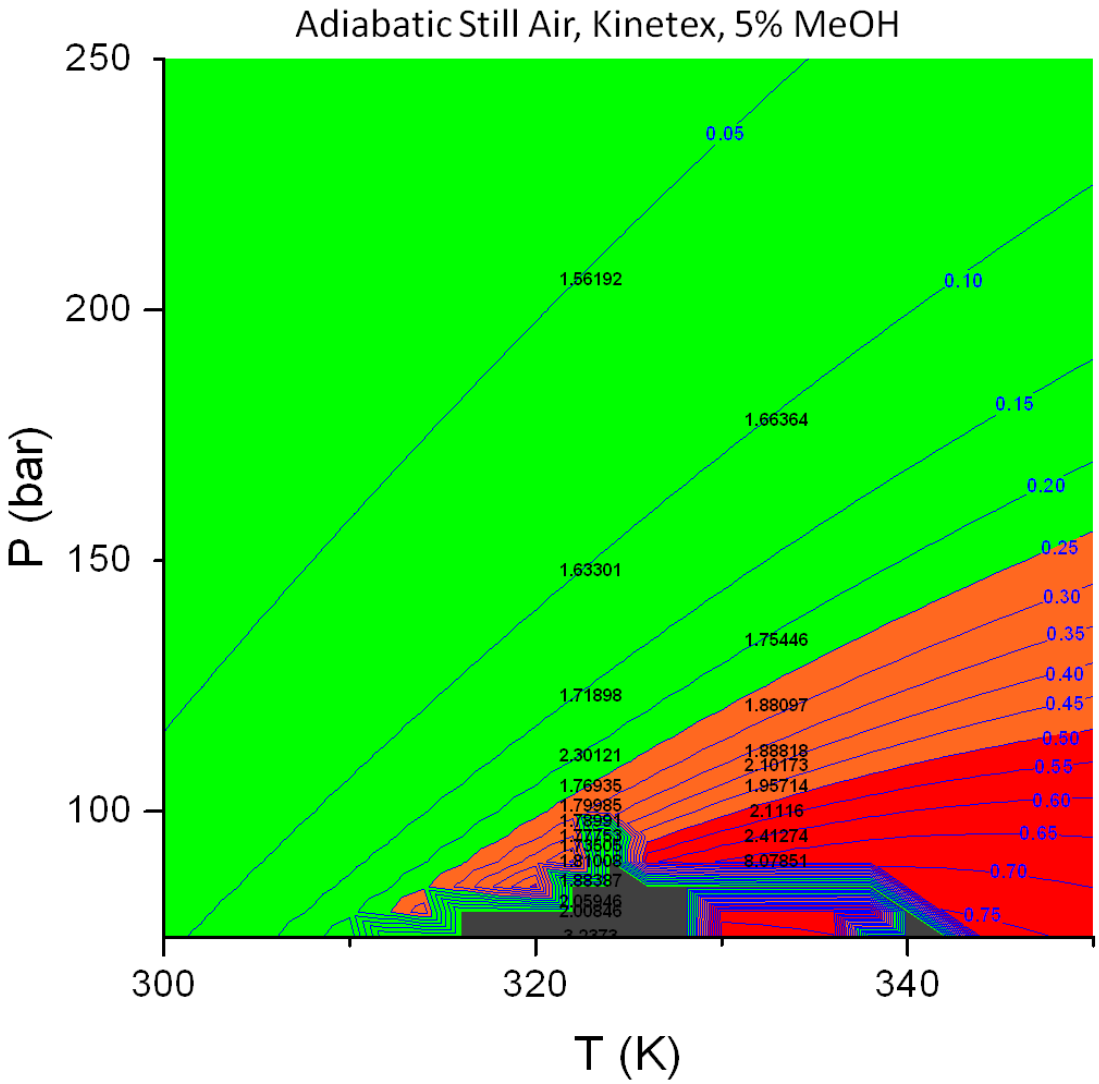

Figure 25. Efficiency for octadecylbenzene on the Kinetex column in adiabatic mode. The blue contours are the Joule Thomson coefficient (K/bar), and the black numbers are the apparent plate height at the corresponding temperature and pressure. The green region represents no efficiency loss, the orange region represents moderate efficiency loss (<25%) and the red region represents excess efficiency loss (>25%).

For the Kinetex column there is no significant efficiency loss at 40 ^{o}C in isothermal still air, Figure 24. In adiabatic mode, larger JT-coefficients are accessible at 50 ^{o}C and 60 ^{o}C before efficiency begins to deteriorate, Figure 25. At 40 ^{o}C in isothermal still-air and 50 ^{o}C in adiabatic mode, chromatographic results were obtained down to outlet pressures where there was no obvious phase transitions occurring at the detector. If the outlet pressure was decreased further, an extremely noisy baseline resulted. There is about 40-cm of 0.007" I.D. tubing connecting the Pout transducer to the UVD. Decreasing this length of tubing may allow even lower outlet pressures to be accessible at 40 and 50 ^{o}C in adiabatic mode, by decreasing the pressure drop between the column outlet and detector. At 60 ^{o}C, retention becomes very strong at outlet pressures below 100 bar, which may lead to additional efficiency loss [10]. No excessive detector noise was observed before efficiency began to deteriorate at 60 ^{o}C. This low pressure limit could be due to a number of things: an inability to match the actual temperature profile of the mobile phase along the column and poor heat transport inside of the column, axial variations in the retention factor along the column [10], or due to operating near the two phase region of the mobile phase [40]-[41]. These will be discussed further in sections 3.5 and 3.6.

3.3 Optimizing the Thermal Environment in the Dual-Zone Tube-Heater

The outlet temperature was varied systematically at a JT-coefficient of 0.40 K/bar at 50 and 60 ^{o}C, 93 bar and 109 bar outlet pressure respectively. The plate height was plotted verses the difference between the measured on column temperature and the adiabatic temperature in Figure 26. The plate height goes through a minimum where the measured temperature minus the adiabatic temperature is equal to 0.0 to 0.2 ^{o}C at 50 and 60 ^{o}C. Operating the column in an environment where the measured outlet temperature is less than or greater than the predicted adiabatic temperature causes the plate height to increase. This means that only small deviations from the adiabatic temperature profile results in significant increases in the plate height under these conditions. Given this, it is possible that further optimization of the thermal environment temperature distribution

may improve efficiency at outlet pressures where efficiency was shown to degrade in this study.

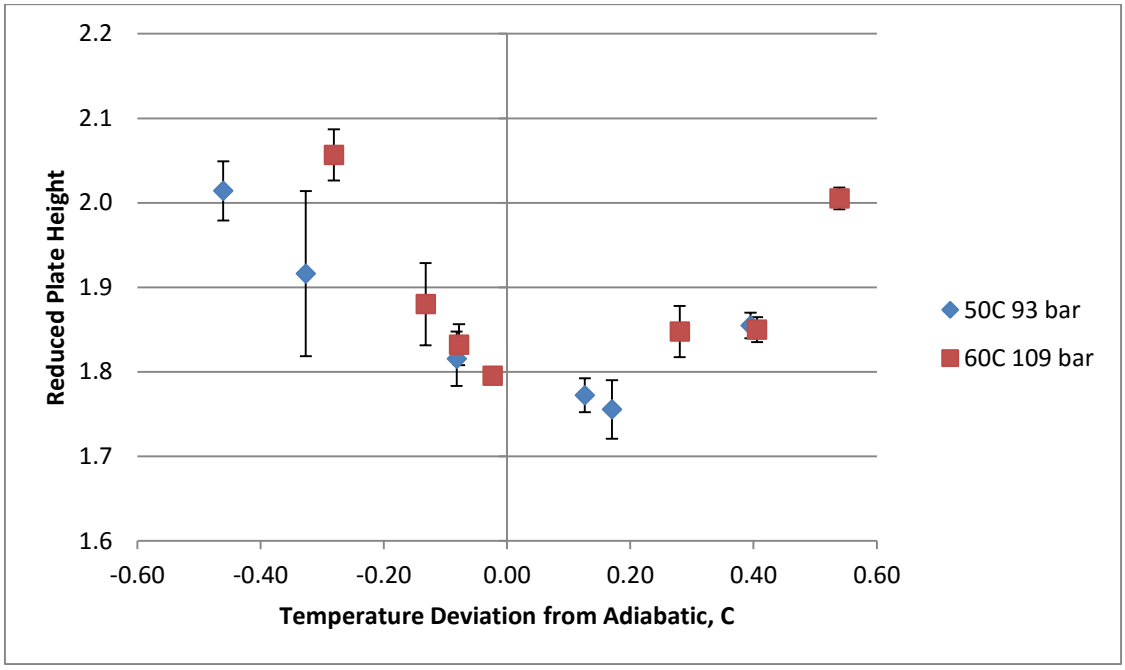

Figure 26. Optimizing the measured column outlet temperature for the Kinetex column at a JT-coefficient of 0.40 K/bar and flow rate of 4.5mL/min. The plate height goes through a minimum when the measured on column temperature is near the predicted adiabatic temperature of the mobile phase inside of the column. Error bars represent the relative standard deviation in the calculated plate height.

3.4 Performance of the Luna Column in Forced-Air and Adiabatic Thermal Environments

Similar behavior was observed, going from forced-air to adiabatic mode for the Luna column used in this study, Figure 27 and Figure 28. At 50 ^{o}C, excess efficiency loss occurred at outlet pressures between 93 and 100 bar, a JT-coefficient between 0.4 and 0.3 K/bar respectively. At 60 ^{o}C, efficiency loss occurred between 116 and 136 bar outlet pressure and JT-coefficients of 0.2 and 0.3 K/bar. Retention on the Luna column is higher than that of the Kinetex under the same operating conditions. This combined with a lower thermal conductivity for fully porous particles compared to superficially porous particles helps explain why the Luna column doesn't perform as well at larger JT-coefficients

compared to the Kinetex column [33]. Still, operating the Luna column adiabatically significantly improves performance under low density conditions.

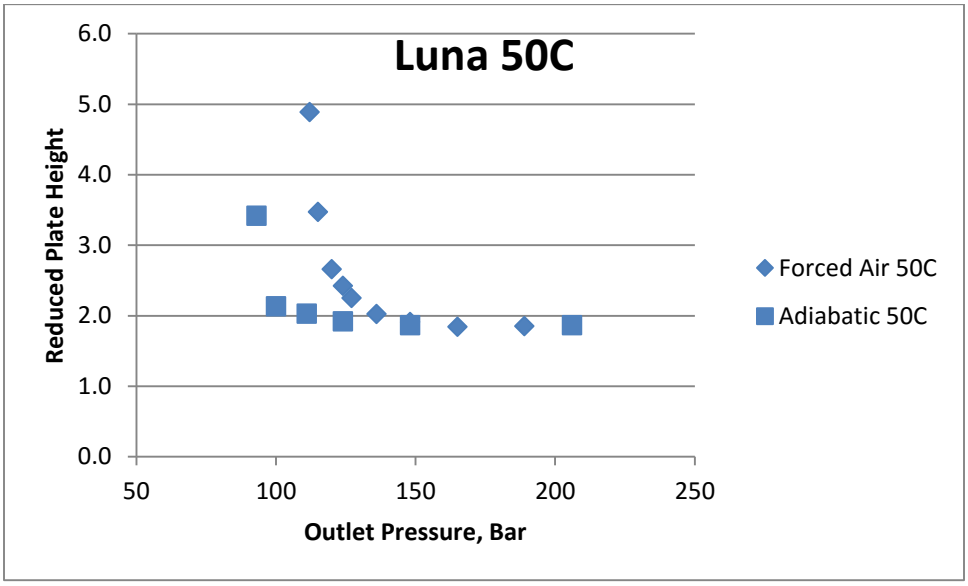

Figure 27. Effect of the thermal environment on efficiency at 50 °C for the Luna column.

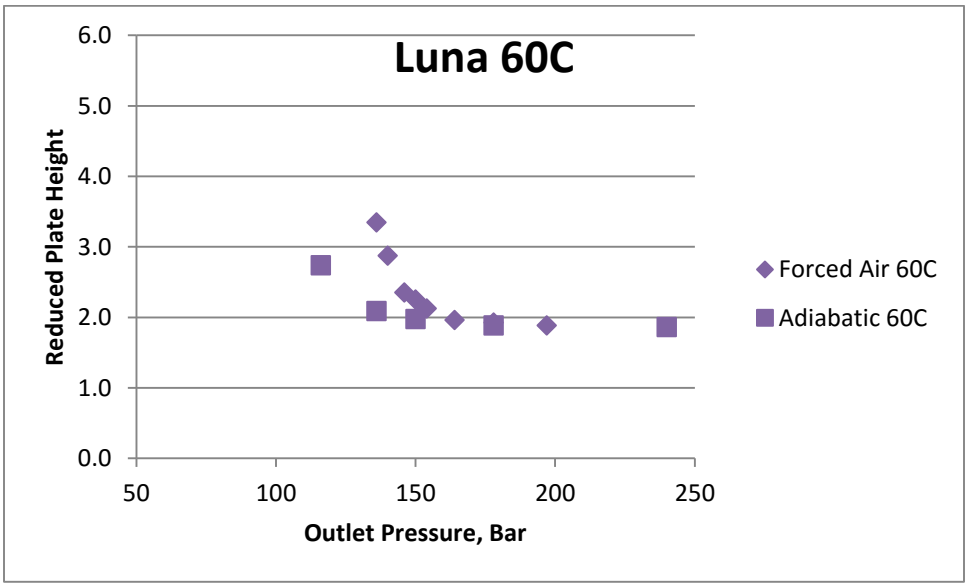

Figure 28. Effect of the thermal environment on efficiency at 60 °C for the Luna column.

3.5 Effect of Axial Gradient in the Retention Factor on Efficiency

Under low density conditions, retention increases rapidly with decreasing outlet pressure; this was observed for both columns in this study. At low outlet pressures, the outlet of the column

experiences very different conditions compared to the inlet of the column. The temperature and density are different near the outlet, which in turn can cause the local retention factor to be different. Axial gradients in the retention factor could result in efficiency loss under some conditions in SFC [10]. Poe and Martire derived a general expression for the apparent (observed) plate height ($\hat{h}$) based on the temporal and spacial averages of the local plate height value (h):

$$\hat{h} = \frac{\left\langle h\left(1+k\right)^2 \rho \right\rangle_t}{\left\langle 1+k \right\rangle_t^2 \left\langle \rho \right\rangle_z} \tag{10}$$

where k is the local retention factor, and t and z denote temporal and spacial averages. Solving this equation requires knowledge about how the retention factor varies with the temperature, pressure, and density of the mobile phase for a given column. A retention model for the Luna column used in this study was developed by Kaczmarski *et. al.* [38] of the general form:

$$k = \exp\left(c_0 + \frac{c_1}{T_r} + c_2 \rho_r + c_3 \frac{\rho_r}{T_r} + c_4 \frac{\rho_r^2}{T_r} \right) \tag{11}$$

Where T_r and ρ_r are the reduced temperature and reduced density and C_0 - C_4 are fitting parameters estimated from experimental data.

Simulations were carried out by numerically solving equations 10 and 11 at 100 points along the chromatographic column. A linear pressure drop is assumed, and the local plate height (h) is set equal to the experimental reduced plate height. The apparent plate height ($\hat{h}$) is calculated based on the axial variation of the retention factor, Equation (10). Two thermal modes were modeled for the adiabatic Luna data at 50 ^{o}C. One assumes a perfectly isothermal column with no radial temperature gradients, and the other assumes a perfectly adiabatic column with no radial temperature gradients. First, the outlet pressure was varied at 50 ^{o}C in an isothermal column. At high outlet pressures, >124 bar, there is less than 1% loss in efficiency due to axial gradients and up to 27% at 93 bar. In an adiabatic column, efficiency loss did not exceed 2% under these conditions. The experimental data corresponds to Figure 27. These results are summarized in Table 2.

Another virtual experiment was carried out where the flow rate was varied at a constant outlet pressure of 93 bar and an inlet temperature of 50 ^{o}C. In isothermal mode, efficiency loss increases with the flow rate, up to 45% at 5 mL/min. However, less than 4% efficiency loss is predicted for the column operated perfectly adiabatic. The experimental data for this simulation corresponds to Figure 31. The simulation results are summarized in

Table 3. These simulation results suggest that if the column is operated perfectly adiabatic, efficiency losses due to axial gradients in the retention factor will be negligible under the conditions examined in this study. Interestingly, eliminating radial temperature gradients by operating the column perfectly isothermal could result in significant efficiency losses due to axial gradients in the retention factor.

Table 2. Simulation results for the effect of axial gradients on efficiency for the Luna column operated in perfectly isothermal (ISO) and adiabatic (ADB) modes as the outlet pressure is changed from 206 bar to 93 bar.

	SH3-028-03			SH3-028-01			SH3-024-03		
	Expt	Calc	Calc	Expt	Calc	Calc	Expt	Calc	Calc
Fp	2	2	2	2	2	2	2	2	2
Pout	206	206	206	124	124	124	93	93	93
Pin	226.1	226.1	226.1	141.5	141.5	141.5	109.3	109.3	109.3
Ppump	233	233	233	147	147	147	115	115	115
Tin	50	50	50	50	50	50	50	50	50
Tout	49.1	49.1	49.1	48.1	48.1	48.1	46.4	46.4	46.4
hr	1.865	1.866	1.866	1.920	1.926	1.933	3.419	3.489	4.347
t0	1.222	1.109	1.107	1.140	1.007	0.994	1.138	0.888	0.833
tr	3.788	3.825	3.820	6.570	6.725	6.987	17.525	16.781	27.790
k	2.100	2.447	2.452	4.738	5.681	6.030	14.396	17.897	32.360
Therm		ABD	ISO		ABD	ISO		ABD	ISO
k.in		2.324	2.324		4.998	4.998		13.502	13.502
k.out		2.580	2.592		6.475	7.423		23.877	95.511
hrbar.expt		1.865	1.865		1.920	1.920		3.419	3.419
hrbar.calc		1.866	1.866		1.926	1.933		3.489	4.347
hrcalc/hrexpt		**1.000**	**1.000**		**1.003**	**1.007**		**1.020**	**1.271**

Table 3. Simulation results for the effect of axial gradients on efficiency for the Luna column operated in perfectly isothermal (ISO) and adiabatic (ADB) modes as the flow rate is changed from 1 to 5 mL/min.

	Expt	Calc	Calc	Expt	Calc	Calc	Expt	Calc	Calc
Fp	1	1	1	3	3	3	5	5	5
Pout	93	93	93	93	93	93	95	95	95
Pin	101	101	101	118	118	118	141	141	141
Ppump	103	103	103	130	130	130	172	172	172
Tin	50.09	50.09	50.09	50.04	50.04	50.04	49.98	49.98	49.98
Tout	47.61	47.61	47.61	45.51	45.51	45.51	44.14	44.14	44.14
hr	5.120	5.724	5.169	3.440	4.889	3.542	2.650	3.832	2.755
t0	2.350	1.580	1.662	0.750	0.573	0.614	0.440	0.366	0.389
tr	57.880	80.009	54.500	8.640	14.771	8.477	3.470	5.194	3.342
k	23.680	49.643	31.790	10.550	24.756	12.803	6.920	13.196	7.598
Therm		ISO	ABD		ISO	ABD		ISO	ABD
k.in		26.293	26.293		9.078	9.078		5.038	5.038
k.out		99.398	38.405		97.217	18.355		60.966	11.939
hrbar.expt		5.120	5.120		3.440	3.440		2.650	2.650
hrbar.calc		5.724	5.169		4.889	3.542		3.832	2.755
hrcalc/hrexpt		**1.118**	**1.010**		**1.421**	**1.030**		**1.446**	**1.039**

3.6 Kinetic Performance for Kinetex and Luna Columns

Representative van Deemter curves were generated for various conditions in isothermal still-air and adiabatic still-air for both the Kinetex and Luna columns, Figure 29 and Figure 31. Variations in the B-term of the van Deemter curve and a shift in the optimum flow rate might be explained by a general increase in the solute diffusion coefficient as the outlet pressure is decreased. At high pressures the viscosity of the mobile phase is greater than at low pressures. This decreases the solute diffusion coefficient in the mobile phase and causes less band spreading at low flow rates. As the outlet pressure is decreased, the mobile phase viscosity decreases causing a corresponding increase in the diffusion coefficient and more band spreading at low flow rates. No major changes were observed in the C-term of the van Deemter curves when changing thermal environments, under conditions where radial temperature gradients do not cause efficiency loss.

For the Kinetex column, what appears to be B-term band broadening resulted as the outlet pressure was decreased, Figure 29. This was observed in both isothermal still-

air and adiabatic still-air at 50 and 60 ºC. Decreasing the outlet pressure from 134 bar to 109 bar shifted the optimum velocity from 3.5 to 4.5 mL/min at 60 ºC. At 60 ºC the efficiency loss that was observed in Isothermal mode at 109 bar was largely restored for the Kinetex column when operating the column adiabatically. However, the apparent column efficiency at 109 bar never reached the column efficiency under uniform conditions.

Retention was not altered noticeably for the Kinetex column when going from isothermal still-air to adiabatic still-air at the same operating temperature and pressure, Figure 30. This suggests that the properties of the bulk fluid inside of the column were largely unchanged when removing radial temperature gradients in this case.

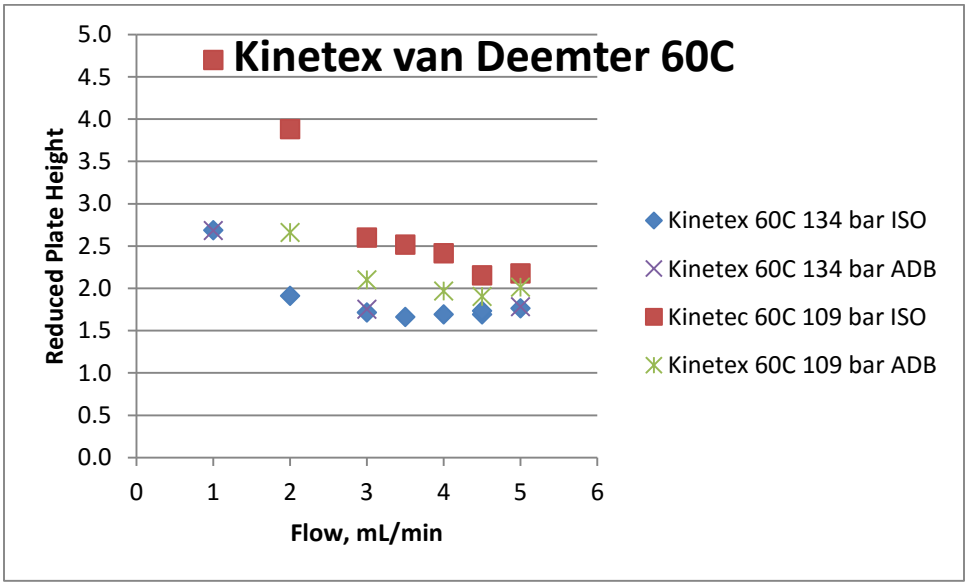

Figure 29. van Deemter curves for the Kinetex column at 60ºC under uniform column conditions (134 bar) and non-uniform conditions (109 bar) in isothermal still-air (ISO) and adiabatic still-air (ADB).

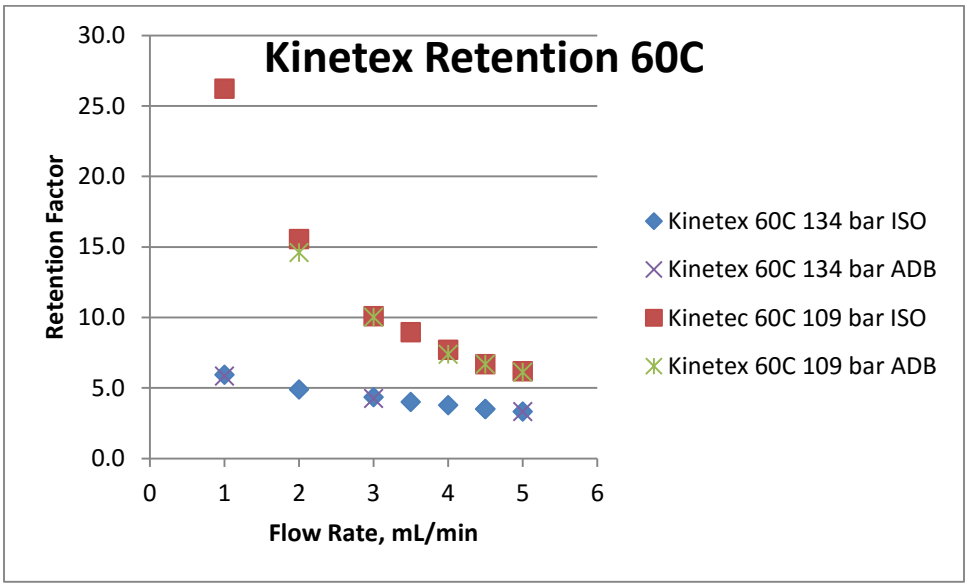

Figure 30. Variations in the retention factor for the van Deemter curves in Figure 29.

Similar van Deemter results were observed for the Luna column, Figure 31. Under uniform conditions, 148 bar, the reduced plate height was 1.87 at an optimum velocity of 2 mL/min. Under non-uniform conditions, 93 bar, what appears to be B-term band broadening is observed and the reduced plate height is 2.65 and still decreasing at a flow rate of 5 mL/min. An optimum flow rate was not observed since the plate height is still decreasing at 5 mL/min.

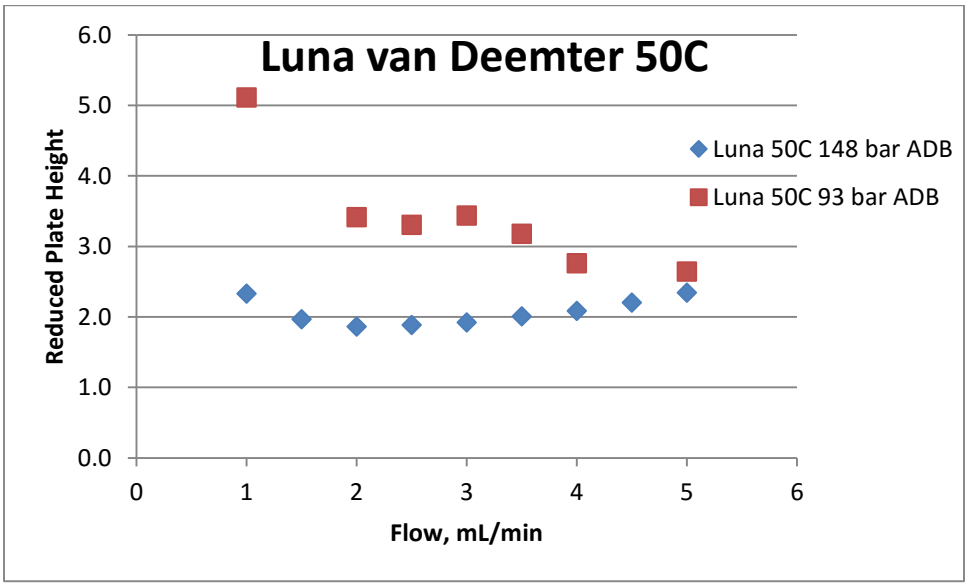

Figure 31. van Deemter curves for the Luna column at 50°C under uniform column conditions (148 bar) and non-uniform conditions (93 bar) in adiabatic still-air (ADB).

The shift in the optimum velocity to higher flow rates may be the result of increased diffusion for the solute. However, the optimum flow rate in SFC is actually dependent on the product of the solute diffusion coefficient (D_m) and the density (ρ). The volumetric flow rate (mL/min) is approximately proportional to the mass flow rate, F_m (Kg/s), and the reduced mobile phase velocity (v) is:

$$v = \frac{F_m d_p}{A \rho D_m} \tag{12}$$

where d_p is the particle size, and A is the cross-sectional area of the column. And according to [37], the product, $\rho\, D_m$, remains approximately constant as the pressure changes. If this approximation is valid at the low outlet pressures in this study, then only marginal shifts in the optimum velocity should be expected. Whether the observed shift for the Kinetex column, from 3 mL/min under uniform conditions to 4.5 mL/min under non-uniform conditions (Figure 29) is actually the result of decreasing the diffusion coefficient is unclear. However, the shift for the Luna column to flow rates greater than 5 mL/min seems unlikely given Equation (12).

Some radial thermal heterogeneity probably remains inside of the column, even in "adiabatic" mode. In this region, high temperatures and low pressures, the heat transport properties of the mobile phase are very poor [24]. Conceptually, large values for thermal diffusivity mean heat is efficiently dispersed and thermal heterogeneity will be minimal. Near the critical point even small temperature differences between the column wall and mobile phase can affect efficiency, since those temperature differences are not evened out due the poor heat transport properties of the mobile phase. This was effectively modeled by Kaczmarski et. al [24][39] for a different solute system on a different column.

We observed similar trends compared to [24] for this chromatography and solute system using a 250-mm X 4.6-mm X 3-μm Luna C18 column. The thermal environment and thermal control was the same as in the still-air set up. The van Deemter curves (Figure 32) appear to show the same behavior as above. Under uniform column conditions the van Deemter curves overlap. At elevated temperature and decreased pressure efficiency is poor at low flow rates and improves at high flow rates.

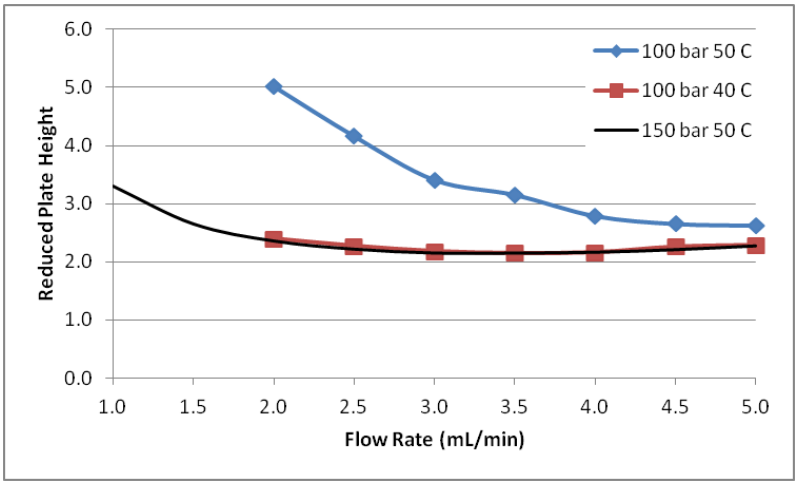

Figure 32. van Deemter curves under uniform and non uniform conditions for a 250mmX4.6mmX3µm Luna C18 column.

This behavior can be explained by plotting the isenthalpic curves on the P-T plane and comparing the thermal diffusivity of the mobile phase to the conditions inside of the column, Figure 33. The red lines are the isenthalpic (adiabatic) curves for the 40 ^{o}C 100 bar van Deemter curve and the blue lines are the isenthalpic curves for the 50 ^{o}C 100 bar van Deemter curve, from Figure 32. The red dashed contours are the thermal diffusivity for the mobile phase (cm^2/s). Focusing on the blue isenthalpic lines (which correspond to the blue van Deemter curve), even though the temperature drop at 5 mL/min is double the temperature drop at 1 mL/min, the plate height at 5 mL/min is about half the plate height at 1 mL/min. The larger plate height at 1 mL/min compared to 5 mL/min may be the result of an inability to curb temperature differences inside of the column due to the lower thermal diffusivity, not variations described by the classic van Deemter curve (5) or Equation (12). Currently it is not possible to obtain good data for the thermal diffusivity of CO_2/methanol mixtures from REFPROP at the low outlet pressures examined for the Kinetex and Luna columns in this study. However, we suspect a similar process is occurring due to an inability to perfectly match the temperature of the column wall to the temperature of the fluid inside of the column. Efficiency is improved using the adiabatic control, but decreasing the outlet pressure further results in even poorer heat transport properties (smaller values for the thermal diffusivity) which amplify any temperature differences between the wall and the fluid inside of the column.

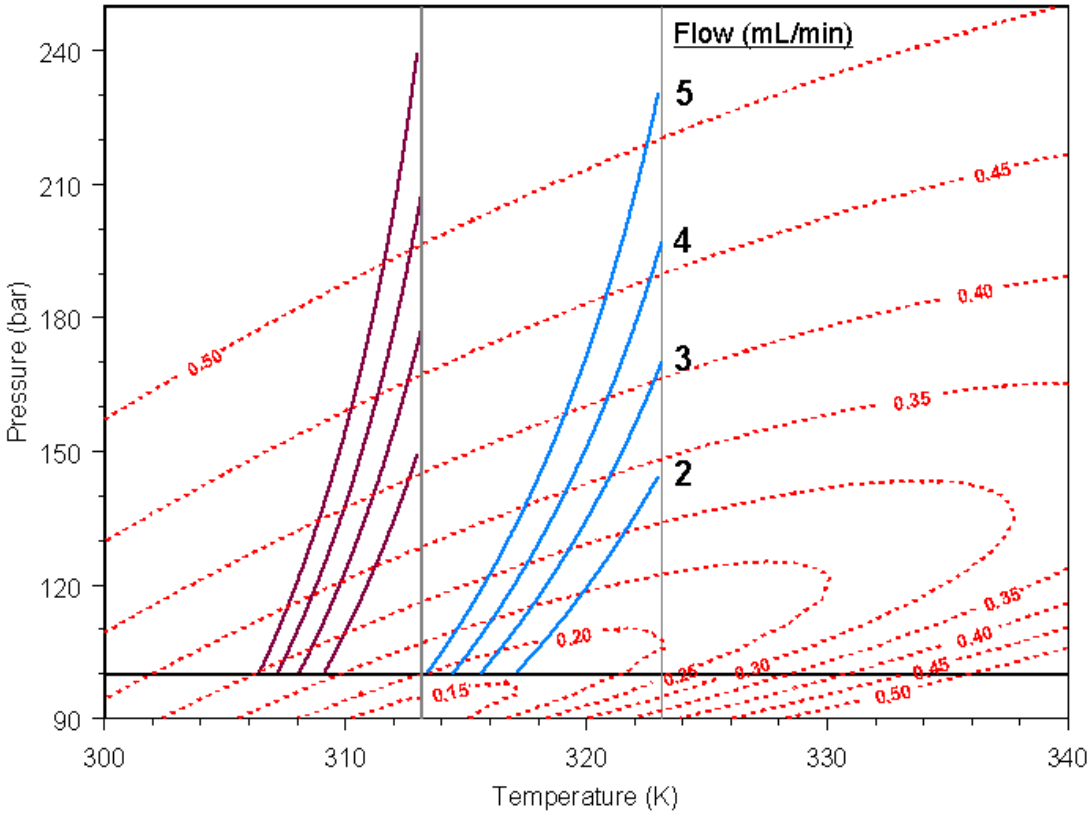

Figure 33. Isenthalpic curves (solid red and blue lines) for the experimental conditions in Figure 32. The outlet conditions (bottom) for the blue curves (50 °C 100 bar) correspond to small values of the thermal diffusivity, 0.15-0.20 cm²/s and poor heat transport. The outlet conditions for the red lines (40°C 100 bar) correspond to larger values for the thermal diffusivity, 0.25-0.30 cm²/s and better heat transport.

It is still possible that the efficiency loss observed in adiabatic mode is due to processes other than thermal heterogeneity caused by poor heat transport near the critical point however. Berger attributed poor performance in the vicinity of the critical point to adsorption of the CO_2/methanol mobile phase on the silica stationary phase, generating a thick film on the surface of the particles [40]. This would increase retention since the density of the adsorbed mobile phase is much higher than the density of the flowing mobile phase, causing the analyte to partition more into the adsorbed film. The efficiency loss could also be due to phase separation of the mobile phase inside of the column [41]. Both of these processes would limit extending this region further, while a heat transfer problem could probably be overcome. Further analysis should be done in order to fully characterize the phenomena controlling efficiency in this region of the phase diagram.

3.7 Applications

Operating the column adiabatically effectively decreases the lower pressure limit that is attainable in packed column SFC. At low outlet pressures, retention and selectivity are sensitive to changes in temperature and pressure. Following are two short examples demonstrating how operating at low outlet pressures may help solve challenging separation problems. The Kinetex column and tube heater with 5% methanol (v/v) mobile phase were used for both applications.

3.7.1 Pressure Ramp Alkylbenzenes

Pressure, or density programming was common early on in capillary SFC however it is rarely used in the recent literature and few applications have been shown using packed columns. This may be because under common operating conditions, retention and selectivity do not change very much with pressure. Much more common is the use of modifier gradients to obtain the needed resolution. However, after running a modifier gradient, there is some downtime between runs to re-equilibrate the column at the initial condition. Pressure changes on the other hand are almost instantaneous inside of the column, so resetting the column after a pressure programmed run is much faster compared to a modifier gradient.

A mixture of n-alkylbenzenes (C2, C4, C6, C8, C10, C12, C14, C16, C18) was separated in less than 3 minutes using a pressure programmed run on the Kinetex (C18) column at 3mL/min and 5% (v/v) methanol mobile phase and 60 ^{o}C inlet temperature. An isobaric separation at 150 bar outlet pressure was unable to resolve C2-C8. Decreasing the outlet pressure to 95 bar resolved all components in the mixture, but took almost 5 minutes to elute C18, Figure 34. A method was set up that held the outlet pressure at 95 bar for 1 minute then started a 40 bar/min pressure ramp to 150 bar. The early eluters (C2-C8) were resolved at 95 bar and then the density was increased to get the late eluters (C10-C18) off of the column. This shortened the method time by almost 50%, compared to the isobaric separation while maintaining resolution for all components in the mixture.

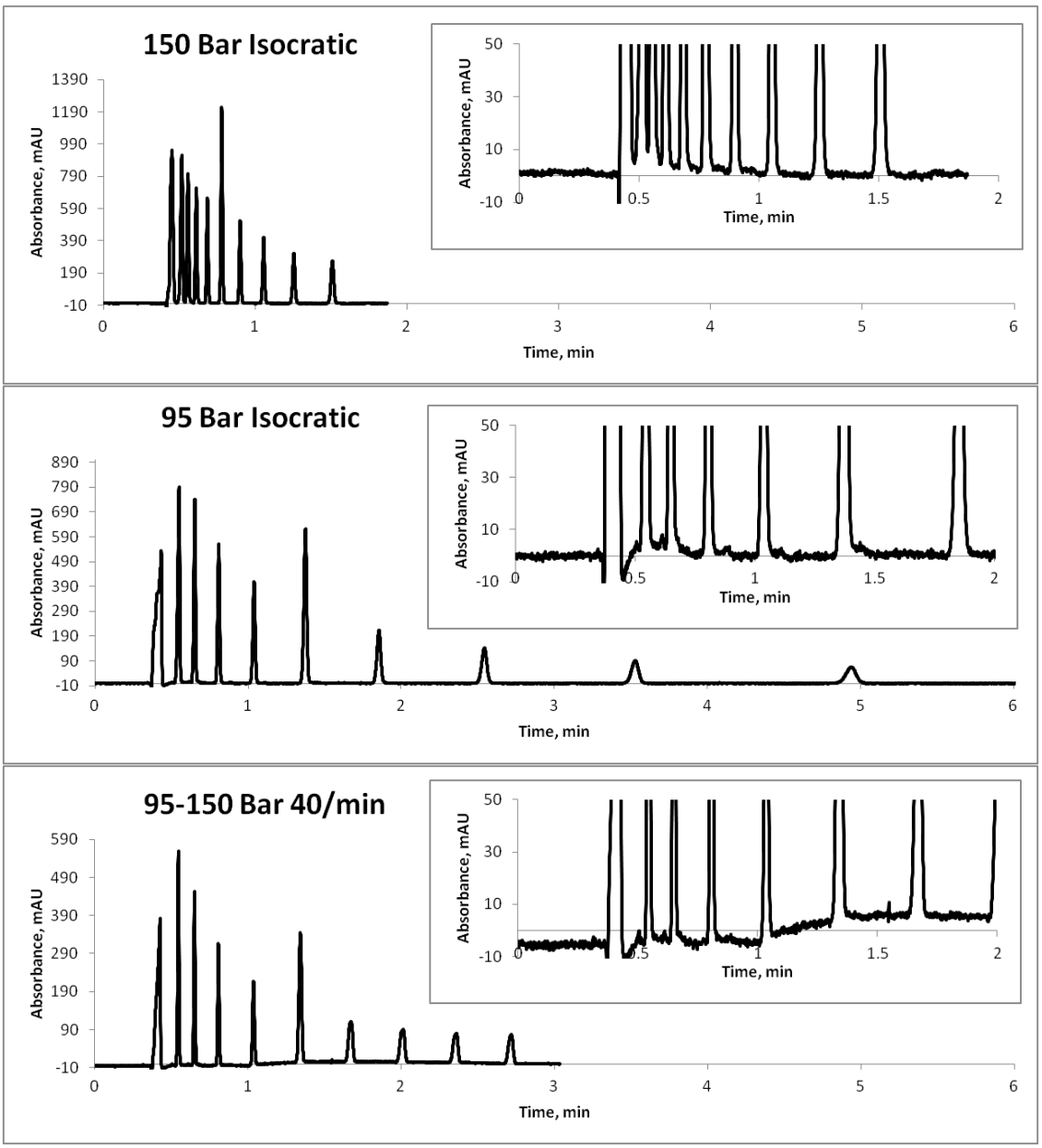

Figure 34.Separation of a homologous series of 9 alkylbenzenes (C2-C18) at 60 °C and 5% MeOH modifier. Top, 150 bar isobaric separation; inset shows a lack of baseline resolution for the early eluters (C2-C8). Middle, 95 bar isobaric separation; inset shows baseline resolution for early eluters. Bottom, pressure programmed run (hold 1 min at 95 bar, ramp to 150 bar at 40 bar/min, hold for 1 minute.

3.7.2 Selectivity of Natural Products

Outlet pressure and operating temperature are important operating parameters in SFC method development, however there are not many examples of how pressures and temperatures are selected for various applications. Again, this may be due to the fact that selectivity doesn't change much with pressure in the current perceived safe zones of operation. Here, a mixture of three natural products, A, B and C, are analyzed on the Kinetex column at 50 ^{o}C 150 bar, 120 bar and 95 bar and a flow rate of 4.5 mL/min, Figure 35. At 50 ^{o}C, compound A is well separated from compounds B and C, which co-elute. At 150 bar, a slight shoulder (impurity) is evident coming off of compound A. Decreasing the outlet pressure to 95 bar almost fully resolves the impurity. At 95 bar, increasing the temperature to 60 ^{o}C is able to fully resolve the impurity from compound A, and compounds B and C begin to separate. This shows how decreasing the outlet pressure and increasing the operating temperature can be used to improve selectivity in SFC in the low pressure supercritical region.

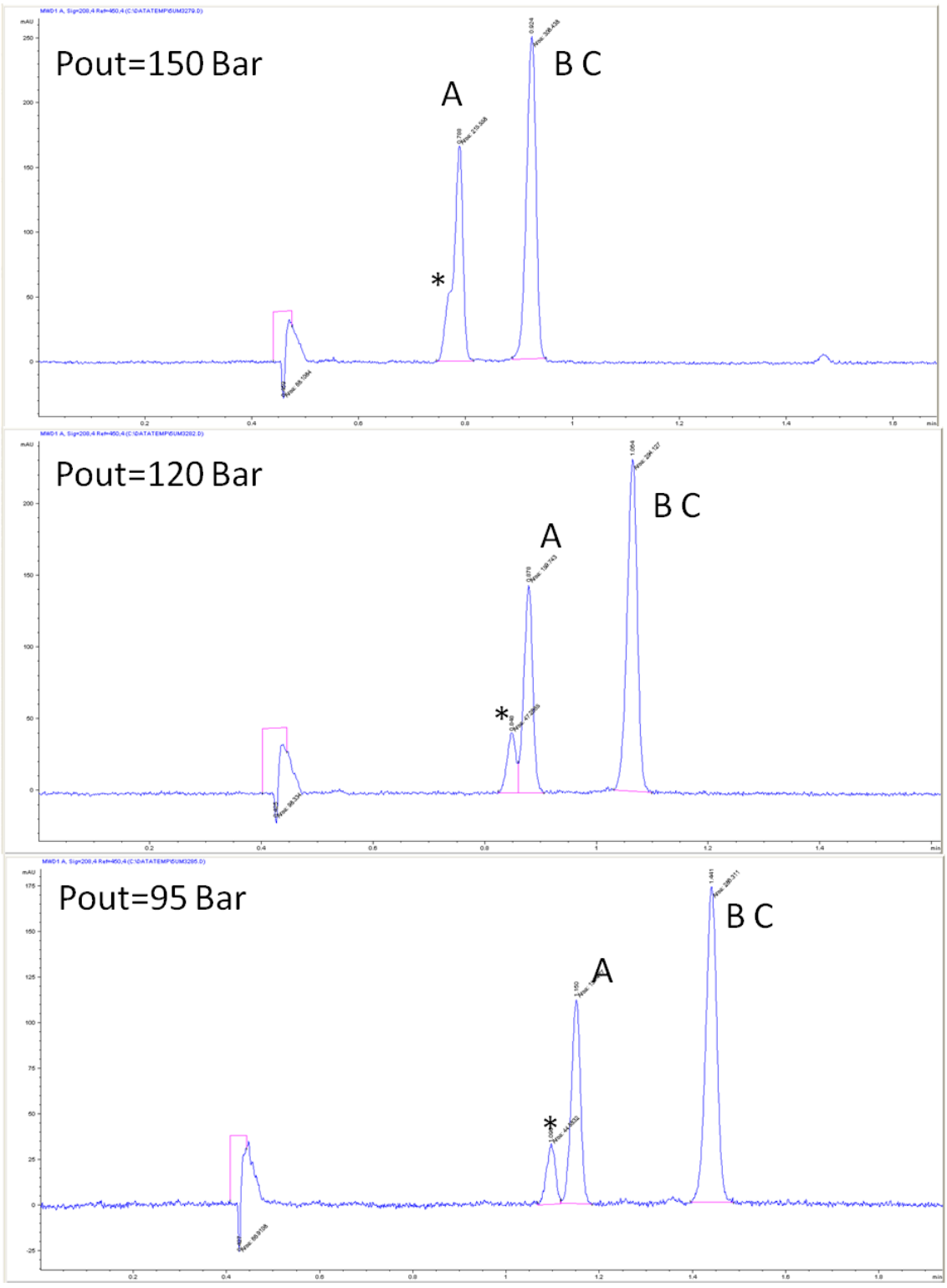

Figure 35. Separation of three natural products, A, B, and C on the Kinetex column at 50 °C and a flow rate of 4.5 mL/min. 150 bar outlet pressure (top), 120 bar outlet pressure (middle), and 95 bar outlet pressure bottom. Compound A is nearly resolved from the impurity (*) at the low outlet pressure.

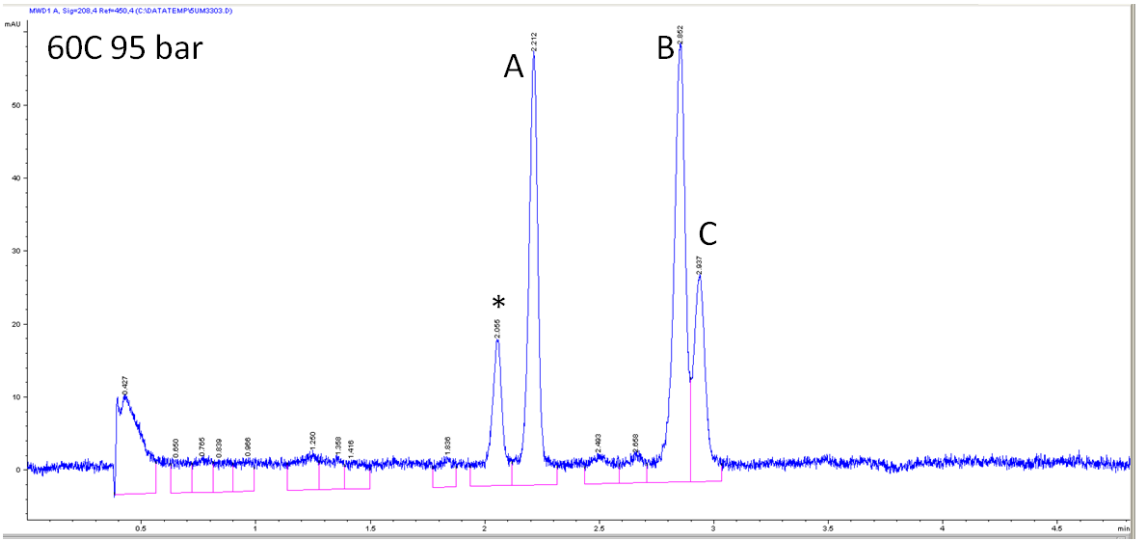

Figure 36. Same separation as Figure 35, except at 60 °C. Baseline resolution of the impurity is obtained, and compounds B and C begin to separate.

4. Conclusion

Significant improvements in column performance were made under low density conditions in the supercritical region by operating the column adiabatically, compared to isothermally in forced-air and still-air. The improvement in efficiency was due to further decreasing the magnitude of the radial temperature gradients that form in packed column SFC as the result of isenthalpic cooling of the mobile phase. A novel approach was developed and tested for thermostatting the column that allowed nearly adiabatic operation. Traditionally, the mobile phase and column temperatures are controlled along with the outlet pressure and the flow rate. The new column heater adds an additional control parameter that allows the practitioner to control the outlet temperature of the column more or less independently from the inlet temperature, and a simple method for determining the outlet setting for the column heater was presented. Operating the column adiabatically allowed our lab to start exploring a region of the phase diagram where retention and selectivity are very sensitive to changes in temperature and pressure.

Losses in efficiency still occurred using this improved thermal mode at even lower pressures and higher temperatures. Based on retention and efficiency modeling results for octadecylbenzene, the efficiency loss does not appear to be due to axial changes in the retention factor. In a perfectly adiabatic environment, efficiency loss should be minimal (<2%) under the conditions examined. The efficiency loss observed in adiabatic mode is possibly due to slight thermal mismatches along the column and poor heat transport, resulting in radial temperature gradients. However, the possibility of efficiency loss resulting from operating near the two phase region of the mobile phase was not examined.

Direct on-column temperature control may be required in order to achieve a perfect adiabatic temperature profile along the column and eliminate radial temperature gradients completely since there are mismatches in the thermal conductivity of the column wall, packed bed, and mobile phase. Preliminary modeling results suggest that removing radial temperature gradients by operating the column perfectly isothermal could result in significant efficiency losses as well.

Literature Cited

[1] Lemmon E., M. Huber, M. McLinden, NIST Reference Thermodynamic and Transport Properties RFPROP, Version 9.0, Physical and Chemical Properties Division, National Institute of Standards and Technology, U.S. Department of Commerce, Boulder, CO 80305 USA, (2011).

[2] E. Lesellier, C. West, Journal of Chromatography A 1382 (2015) 2.

[3] T.A. Berger, Instrumentation for analytical scale supercritical fluid chromatography, J. Chromatogr. A, (2015).

[4] L. Zeng, R. Xu, Y. Zhang, D.B. Kassel, Journal of Chromatography, A 1218 (2011) 3080.

[5] A. Tarafder, G. Guiochon, Journal of Chromatography A 1265 (2012) 165.

[6] J.C. Giddings, Unified Separation Science, Wiley & Sons: New York, NY (1991)

[7] S. R. Allada, Ind. Eng. Chem. Des. Dev. 23 (1984) 344.

[8] T.L. Chester, Microchemical Journal 61 (1999) 12.

[9] Unified Chromatography, J.F. Parcher, T.L. Chester, ASC Symposium Series 748, American Chemical Society: Washington, DC (2000)

[10] D.P. Poe D.E. Martire Journal of Chromatography 517 (1990) 3.

[11] F. Gritti G. Guiochon, Journal of Chromatography A 1295 (2013) 114.

[12] A. Tarafder, G. Guiochon Journal of Chromatography A 1229 (2012) 249.

[13] P.J. Schoenmakers, L.G.M. Uunk, Chromatographia 24 (1987) 51.

[14] T.A. Berger, J.F. Deye, Chromatographia 30 (1990) 57

[15] T. A. Berger, L.M. Blumberg, Chromatographia 38 no.1/2 (1994) 5.

[16] A. Tarafder, G. Guiochon, Journal of Chromatography A 1218 (2011) 4569.

[17] A. Tarafder, G. Guiochon, Journal of Chromatography A 1218 (2011) 4576.

[18] A. Tarafder G. Guiochon Journal of Chromatography A 1218 (2011) 7189.

[19] A. Tarafder, K. Kaczmarski, M. Ranger, D. P. Poe, G. Guiochon, Journal of Chromatography A 1238 (2012) 132.

[20] A. Tarafder, K. Kaczmarski, D.P. Poe, G. Guiochon, Journal of Chromatography A 1258 (2012) 136.

[21] D.P Poe, Journal of Chromatography A 785 (1997) 129.

[22] D.P. Poe J.J. Schroden Journal of Chromatography A 1216 (2009) 7915.

[23] J. Zauner, R. Lusk, S. Koski, D.P Poe, 1266 (2012) 149.

[24] K. Kaczmarski, D.P. Poe, A. Tarafder, G. Guiochon, Journal of Chromatography A 1291 (2013) 155.

[25] D.P. Poe *et.al.* Journal of Chromatography A 785 (1997) 135.

[26] D.P. Poe, D. Veit, M. Ranger, K. Kaczmarski, A. Tarafder, G. Guiochon, Journal of Chromatography A 1250 (2012) 105.

[27] K. Kaczmarski, D.P. Poe, A. Tarafder, G. Guiochon, Journal of Chromatography A 1250 (2012) 115.

[28] D.P. Poe, D. Veit, M. Ranger, K. Kaczmarski, A. Tarafder, G. Guiochon Journal of Chromatography A 1323 (2014) 143.

[29] A. Tarafder, P. Iraneta, G. Guiochon, K. Kaczmarski, D.P. Poe, 1366 (2014) 126.

[30] H. Poppe, J.C. Kraak, J.F.K. Huber, J.H.M. van den Berg, Chromatographia 14-9 (1981) 515.

[31] R. De Pauw, K. Choikhet, G. Desmet, K. Broeckhoven Journal of Chromatography A 1365 (2014) 212.

[32] S.O. Colgate, T.A. Berger, Journal of Chromatography A 1385 (2015) 94.

[33] D.P. Poe, S.C. Helmueller, S. Kobany, H. Feldhacker, Manuscript in Preparation (2016)

[34] F. Gritti, G. Guiochon, Journal of Chromatography A 1138 (2007) 141.

[35] K. Broeckhoven, G. Desmet *et.al.* Journal of Chromatography A 1217 (2010) 2022.

[36] J.J. Li, K.B. Thurbide, Canadian Journal of Analytical Sciences and Spectroscopy 51-4 (2006) 187.

[37] D.P. Poe, Journal of Chromatography A 1078 (2005) 152.

[38] K. Kaczmarski, D.P. Poe, G. Guiochon 1218 (2011) 6531.

[39] M. Lesko D.P. Poe, K. Kaczmarski, Journal of Chromatography A 1305 (2013) 285.

[40] T.A. Berger, Chromatographia 37 (1993) 645.

[41] T.A. Berger, Chromatographia 31 (1991) 529.